STUDIES ON NOVEL FERROELECTRIC LIQUID CRYSTALLINE COMPOUNDS CONTAINING FLUORENE AND FLUORENONE SKELETONS

KOHKI TAKATOH
Display System Laboratory
Research and Development Center
Toshiba Corporation
1992

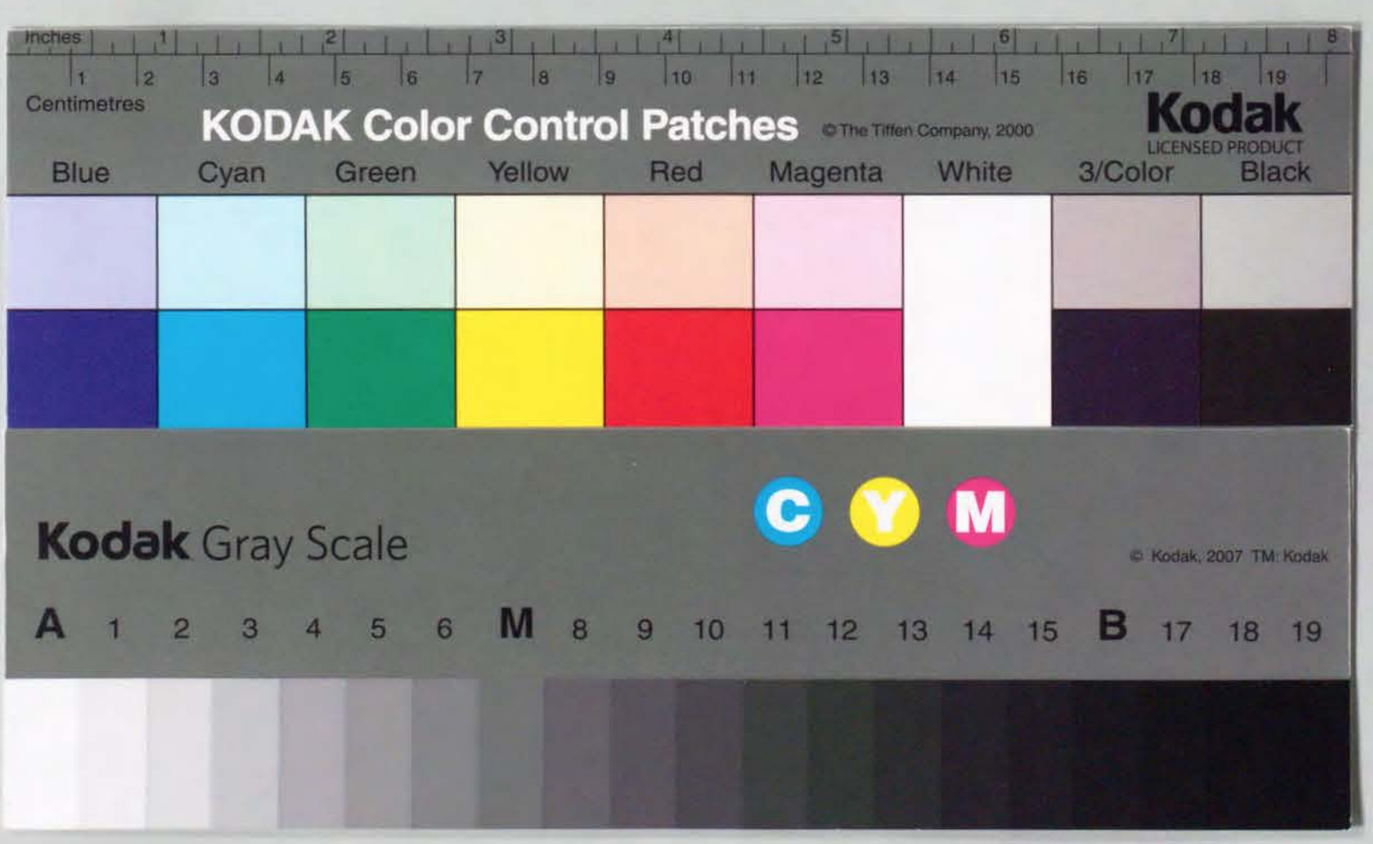

CONTENTS

Chapter 1 General Introduction

Part 1 Liquid Crystal and Aromatic Organic Chemistry

The purpose of this research was to investigate the relationship among chemical structure of molecules, properties for each compound and behaviors as display materials in the liquid crystal field.

Liquid crystals are organic materials with special chemical structures, which show fluidity and certain structural order. They are intermediate states between liquid states and crystal states[1]. "Special chemical structures" mean those with rigid and long central cores, such as aromatic structures, and with alkyl groups in one end or in both ends. In these "central cores", called mesogens, two or three aromatic structures or cyclohexyl rings are combined by some linkages, such as single, double, triple, ester, ether linkage and so on. Usually, aromatic structures are relatively simple ones, such as phenyl, naphthyl and biphenyl groups. Aromatic structures, containing heteroatoms, such as pyridine and pyrimidine structures, have also been contained on several occasions[2].

Most properties of liquid crystalline materials are determined by chemical structures for mesogen parts. Therefore, research on liquid crystalline compounds aroused the interest of organic chemists who are always interested in the structures and properties of organic compounds, especially aromatic organic compounds.

It is well known that there are many kinds of crystal structures. In the field of liquid crystalline materials, there are also several kinds of phases, such as nematic phase and smectic A, B, C, D, E, F, G, H phases[3]. They can roughly be divided into two categories, nematic phase and smectic phases. In nematic phase, there is no layer structure. On the other hand, in smectic phases, there are several kinds of layer structures. Smectic phases can be grouped into 8 classes. Smectic phases have higher structural order than nematic phase. So, smectic phases can be said to have structures close to those for crystals.

It can be easily expected that compounds with mesogen structures with extended system, especially π-electron system, tend to show smectic phases of

high order. In the case of smectic liquid crystals, flexibilities of molecular modification are increased and large varieties of molecular structures, especially aromatic structures, in the part of mesogen, become possible and the molecular structural changes vividly reflect the properties of the compound. Therefore, smectic liquid crystal is an attractive research subject, from the view point of aromatic organic chemistry[3].

However, smectic liquid crystals had hardly been investigated from a practical view point up to about ten years ago. The reason is that practical liquid crystal devices have adopted the modes using nematic liquid crystals, such as a twisted nematic liquid crystal device. Nevertheless, smectic liquid crystals, especially chiral smectic C phase, which can be used as ferroelectric liquid crystalline materials, have received increasing interest, since the discovery of ferroelectric liquid crystals by Meyer et al[4] in 1975 or the proposal of surface stabilized ferroelectric liquid crystals by Clark and Lagarwall[5] in 1980. As described later, practical use has been intensely anticipated for this mode, because of its

quick response and memory property.

The author undertook research and development on ferroelectric liquid crystalline materials in 1986. In that period, ferroelectric liquid crystal had gradually achieved popularity. However, materials able to be used were still quite limited. Therefore, the author determined to enter upon study with the design for a novel ferroelectric liquid crystalline materials[6].

Although constrained to obtain new ferroelectric liquid crystalline materials of high efficiency, the author desired to demonstrate the relationships among chemical structures of molecules, properties of liquid crystalline compounds and further their behaviors as materials for liquid crystal devices. That is , the author intended to carry out molecular modifications, which are simplest and most meaningful in the view of structural organic chemistry.

Before presenting an explanation of the author's molecular design, ferroelectric liquid crystal should be explained.

Part 2 Ferroelectric Liquid Crystal Display

1 Introduction

In 1975[4], ferroelectric liquid crystal was confirmed by Meyer et al using (S)-2-methylbutyl-p-(-p-n-decyloxybenzylideneamino)cinnamate, which was designed and synthesized according to their own theory.

In 1980[5], surface stabilize ferroelectric liquid crystal display was discovered by Clark and Lagerwall. This kind of display drew intense attention, both regarding basic research and applications for its high response time (scores of microseconds) and memory property. Practically, this display was expected to be used for a large flat display panel. This ferroelectric liquid crystal display has been one of the most actively investigated liquid crystal display modes.

2 Structures of Liquid Crystal Phases

There are several kinds of liquid crystal phases. Typical liquid crystal phases are shown in Fig.1. The simplest one is nematic phase. This phase

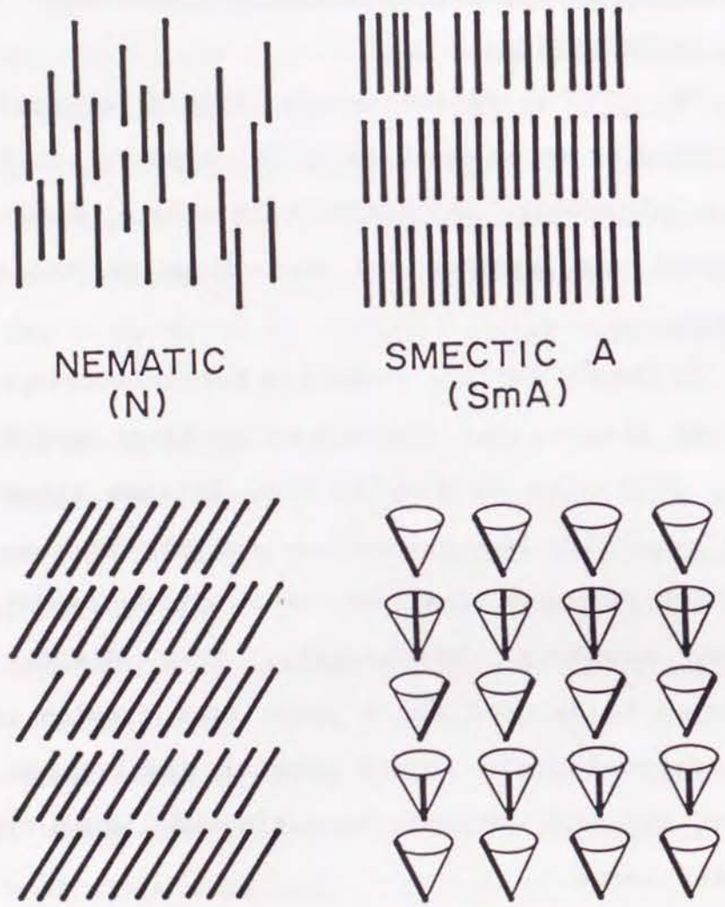

FIGURE 1 The Structural Classification of Liquid Crystals

has been used in almost all liquid crystal displays, twisted nematic liquid crystal display (TN-LCD) or supertwisted liquid crystal display (STN-LCD). In this kind of liquid crystal phase, molecules align in one direction, but there is no other order. On the other hand, there are layer structures in smectic phases. There are many kinds of smectic phases, like A, B, C, D, E, F and G.

In the smectic A phase, the molecules align parallel to the layer normal. Smectic A phase is the simplest among smectic phases.

In the smectic C phase, molecules decline some degrees (tilt angle) to the nomal line of the layer. If chiral structure is introduced to the molecules, showing smectic C phase, a helical structure appears, like that in Fig. 1 (chiral smectic C phase). This liquid crystal phase is called chiral smectic C phase. In ferroelectric liquid crystal display, materials which show this chiral smectic C phase are used.

3 Structure and Mechanism of Ferroelectric Liquid Crystal Display

Figure 2 shows, a cell, filled by liquid crystalline material showing chiral smectic C phase. The surfaces of two plates are treated to align liquid crystalline molecules in parallel. These surfaces are called the alignment layer. Liquid crystalline molecules align in parallel direction with helical structure, as mentioned above. In the figure, the arrows show the dipole moment perpendicular to the molecules.

When the distance between the two plates is made less than several microns, the helical structure disappears, and only two states, in which the dipole moment is fixed to the upper side or to the lower side, perpendicular to the surface of the planes, become stable due to the interaction between liquid crystalline molecules and alignment layers. Electric polarization in unit area without electric field is called spontaneous polarization. These two states can be interchanged by applying an electric field perpendicular to the plane. In ferroelectric liquid crystal display, this molecular movement by electric field is

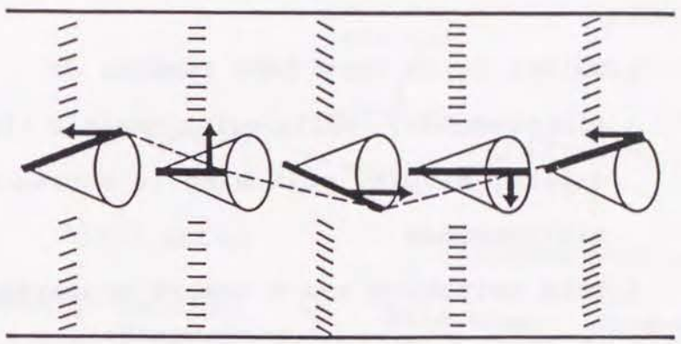

FIGURE 2 The Structure and The Mechanism of Ferroelectric Liquid Crystal

used for switching light.

This ferroelectric liquid crystal display has two features.

1. Switching is very fast (scores of microseconds), while twist nematic liquid crystal display switching is scores of milliseconds.
2. This switching has a memory property.

PART 3 Ferroelectric Liquid Crystalline Materials

1 Introduction

As described above, the ferroelectric liquid crystal is also an interesting subject for organic synthesis, because of its flexibility in molecular modification and the vivid reflection of molecular structural change to its properties.

Features of molecular structures and the basic concept for molecular design[6], adopted by the author, will be explained in detail.

2 Molecular Structural Features for Ferroelectric Liquid Crystalline Materials

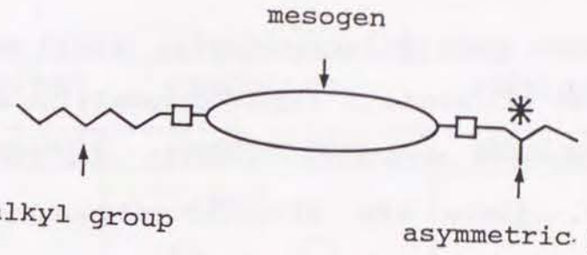

FIGURE 3 Feature of Molecular Stracture of Ferroelectric Liquid Crystal

Figure 3 illustrates an outline of the molecular structure for ferroelectric liquid crystalline materials. Generally, ferroelectric liquid crystalline molecules consist of three parts.

1. Mesogen part
2. Normal alkyl chain part
3. Asymmetric part

Although the asymmetric part is a necessary element to obtain ferroelectric liquid crystal state, as mentioned above, and the normal alkyl chain is a necessary factor to make liquid crystal states stable, the mesogen part will be discussed in detail, because the relationship between the structure of mesogen part of ferroelectric liquid crystalline

molecules and their properties is the main subject of this research.

3 Mesogen Part of Ferroelectric Liquid Crystals

Almost all kinds of liquid crystalline molecules contain mesogen structure. Usually, in the mesogen structure, there are aromatic structures, like phenyl, biphenyl, phenylpyrimidine structure, or cyclohexane ring[2]. These structures are linked with single bond, ester linkage, ether linkage or other linkages. The mesogen part consists of a rigid structure, in which electron density is high. Therefore, this part determines the intermolecular force between neighboring liquid crystalline molecules.

It is well known that phase transition behavior of liquid crystalline materials is mainly determined by the mesogen structure of liquid crystalline materials. Many other properties of liquid crystalline materials, such as viscosity, elasticity and so on, are also determined by mesogen structure.

J.W.Goodby reported that[6] more than two aromatic rings in mesogen part and strong dipole moment perpendicular to the molecular axis in the terminal

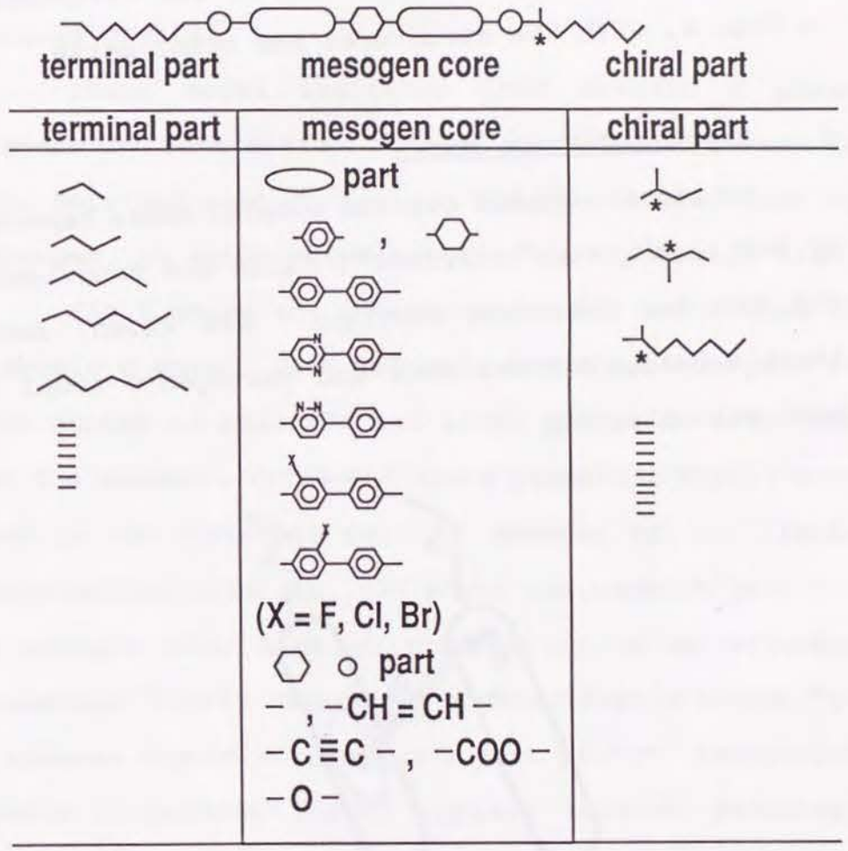

FIGURE 4 Examples of Ferroelectric Liquid Crystalline Molecules

part of mesogen are necessary for thermally stable smectic C liquid crystal phase.

Examples of mesogen structures are illustrated in Fig. 4, with the structures for other parts.

4 Smectic C Phase Model

As smectic liquid crystal models, those reported by McMillan[7], Wulf[8], Priest[9], Calib and Benguigui[10] and Van der Meer and Vertogen[11] are known. Among those models, Van der Meer and Vertogen's model is most reliable.

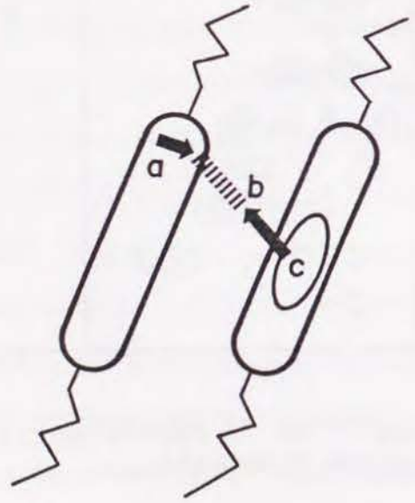

FIGURE 5 Mechanism of the Occurrence of Smectic C Phase

The model by Van der Meer and Vertogen will be discussed in detail, because their model is the starting point for this research on ferroelectric liquid crystal.

Their model indicates that smectic C phase occurs by interaction between the dipole monent in the terminal part of mesogen and the central part of mesogen, in which polarizability is especially high.

Fig.5 shows the mechanism for the occurrence of smectic C phase. Each molecule has a mesogen part in the center of molecule and alkyl groups at both ends of the mesogen. Arrow "a" shows permanent dipole moment in the terminal part of mesogen of one liquid crystalline molecule. "c" shows the central part for a mesogen with high polarizability in an adjacent molecule. Dipole moment "a" induces dipole moment "b" (induced dipole moment) in a part of "c". Attractive force (induction force) appears between permanent dipole moment "a" and the induced dipole moment "b". Molecules decline by this attractive force. The greater this attractive force, the larger the degree of declination (tilt angle).

5 Smectic C Phase Feature

According to Van der Meer and Vertorgen's model, some features of smectic C phase, mentioned below, can be derived.

1. Molecules rotate freely around their molecular axis in smectic A phase and smectic C phase. The rotation does not influence the occurrence of smectic C phase or the induction force.
2. Two dipole moments act independently from the center of polarizability in the adjacent molecule to introduce the induction force.
3. The determination for the position of dipole moment is important for smectic C phase occurrence. Generally speaking, the best position is the terminal part of the mesogen.
4. In the smectic C phase, individual molecules occupy a larger domain in the layer, than in the smectic A phase. So, an increase in molecular volume acts to inhibit smectic C phase occurrence.
5. When the induction force in smectic C phase is strong, the tilt angle becomes large, the

temperature dependence for the tilt angle becomes small and smectic A phase becomes unstable in all the temperature range. In this case, smectic C phase transits the nematic phase or isotropic phase directly, not through the smectic A phase.

6. Smectic C-smectic A transition is a second order transition.
7. When the attractive force between polarizable centers of individual liquid crystalline molecules, which stabilizes smectic A phase, becomes greater than the induction force, which stabilizes smectic C phase, transition from smectic C phase to smectic A phase occurs.

Concerning smectic A phase, McMillan's model[7] explains the stabilization, using the interaction between mesogen parts of large polarizability in liquid crystalline molecules.

PART 4 Molecular Design of Novel Ferroelectric Liquid Crystalline Molecules

1 Introduction

When the author started research on ferroelectric liquid crystal devices and material in 1986, the variation in ferroelectric liquid crystalline materials was still very limited.

The author, a member of Toshiba Corporation R&D Center Chemical Lab., considered that in the development of high efficiency and high reliability for ferroelectric liquid crystal device, it is effective to study molecular design of concrete molecules for ferroelectric liquid crystalline materials, on the basis of the theoretical model of smectic C phase mentioned above, and examine the properties of obtained products to feedback the result into molecular design.

At that time, the most popular mesogen structure was biphenyl structure. Most liquid crystals with biphenyl structure show smectic A and smectic C phases. As the modification of these biphenyl derivatives, the author considered the method mentioned below effective to obtain a wider temperature range

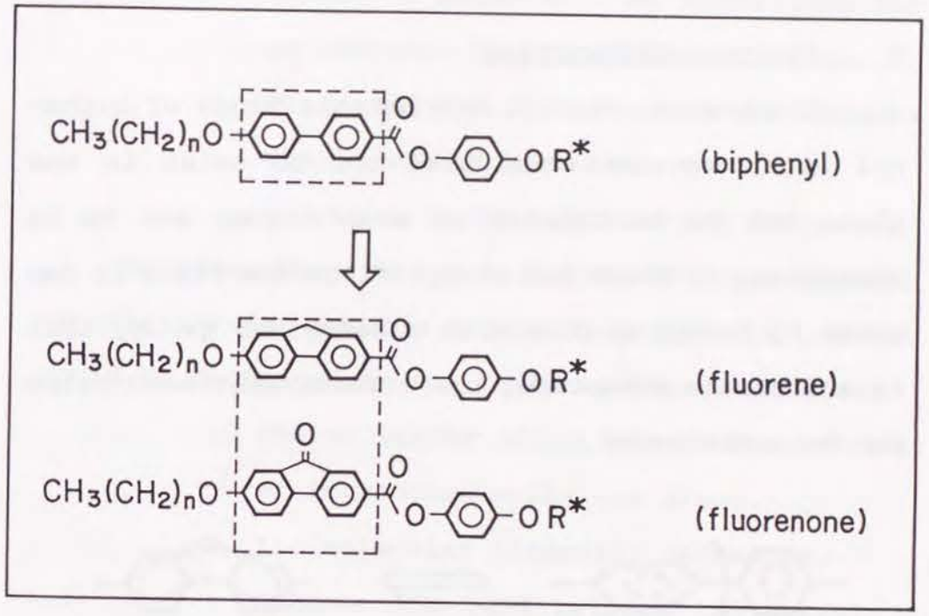

R* =  or 

FIGURE 6 Molecular Design of Fluorene and Fluorenone Derivatives

of smectic C phase, larger tilt angles and larger spontaneous polarization.

2 Fluorene Derivatives

As shown in Fig. 7, two benzene rings of biphenyl structure are considered not to exist in one plane but to be twisted at some degree and to be vibrating. If these two phenyl rings are fixed in one plane by bridging them with a methylene group, that is a fluorene structure, the effects mentioned below can be anticipated.

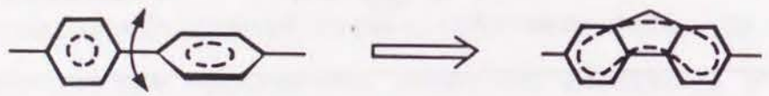

FIGURE 7 Feature of Fluorene Structure

The mesogen part is fixed in one plane. So, π-electrons of two benzene rings are delocalized and the polarizability increases.

As a result,

1. Smectic A phase will be stabilized for an increase in attractive interaction between the mesogen core of neighboring

liquid crystalline molecules, as predicted from McMillan's model.

2. Smectic C phase will be stabilized for an increase in attractive induction force between dipole moment and induced dipole moment in the mesogen part, according to Van der Meer and Vertorgen.

However, there is a possibility that the thermal stabilities for smectic A phase and smectic C phase would be decreased by two factors described below.

1. The molecular width increases, because of introduced methylene group.
2. The molecular linearity decreases, because the bond between two phenyl groups is bent about 24 degrees in the fluorene structure[12].

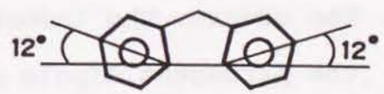

FIGURE 8 Structure of Fluorene Skeleton

Because these two factors decrease the anisotropy for the molecule, the thermal stability of liquid crystal phases could be reduced. Especially, the thermal stability of smectic C phase could decrease.

3 Fluorenone Derivatives

Next, fluorenone derivatives, in which the methylene group of fluorene derivatives is replaced by the carbonyl group, were taken up.

The features below are forseen for fluorenone derivatives.

1. According to Van der Meer and Vertorgen, by introducing the dipole moment for the carbonyl group, perpendicular to the molecular axis, smectic C phase thermal stability would increase.
2. The greater the induction force between the permanent dipole moment and induced dipole moment becomes, due to the dipole moment introduction, the more the molecules decline. So, larger tilt angles and, as a result, larger spontaneous polarization can be expected[13].
3. The molecules become still wider than fluorene derivatives. So, molecular anisotropy become lower. This would decrease the thermal stability of liquid crystal phase, especially of smectic C phase.

Considering these factors, the author started to investigate fluorene and fluorenone derivatives to clarify the relationship between molecular structure and properties of liquid crystalline compounds with the desire to obtain novel ferroelectric liquid crystalline compounds in a wide temperature range of smectic C phase, large tilt angle and large spontaneous polarization.

Reference

1. G. W. Gray: Thermotropic Liquid Crystals, John Wiley & Sons (1987)
2. D. Damus and H. Zashke: Elüssige Kristalle in Tabellen II (1984)
3 K. Takatoh and M.Sakamoto, Kagaku Kogyo, 49 (10), (1989), 881
4. R. B. Meyer, L. Liebert, L. Strzelecki and P. Keller: J. de Phys., 36, (1975) L69
5. N. A. Clark and S. T. Lagerwall: Appl. Phys. Lett., 36 (1980) 899
6. J. W. Goodby and T. M. Leslie, Mol. Cryst. Liq. Cryst., 110 (1984) 175
7. W. L. McMillan, Phys. Rev. A, 8 (1973) 1921
8. A. Wulf, Phys. Rev. A, 11 (1975) 365
9. R. G. Priest, J. Physique, 36, (1975) 437; J. Chem. Phys., 65 (1976) 408
10. D. Cabib and L. Benguigui, J. Physique 38 (1977) 419
11. B. W. Van der Meer and G. Vertogen, J. de Phys. 40, C3-222 (1979)

12. (a) D. M. Burns and J. Iball, Nature, 173 (1954) 635 ; (b) G. M. Brown and M. H. Bortner, Acta Cryst., 7 (1954) 139
13. (a) S. Dumrongrattana and C. C. Huang, Phys. Rev. Lett., 56 (5) (1986) 464; (b) J. S. Patel and J. W. Goodby, Mol. Cryst. Liq. Cryst., 144 (1987) 117

CHAPTER 2 Phase Transition Behavior of Fluorene and Fluorenone Derivatives[1)]

PART 1 Introduction

1 Introduction

Ferroelectric liquid crystals have been the subject of much interest due to their potential advantage in regard to quick response and memory properties in display device application.[2)] However,the variety of materials available for those applications is still limited at present, compared with the well-developed nematic liquid crystalline materials. Further, the relationship between the molecular structures and the properties of the chiral smectic C phase has not been fully clarified yet.

However, many of the mesogens of the ferroelectric liquid crystalline materials reported so far contain a biphenyl structure[3)] in their mesogens. So, the investigation on the effect of the structural modification of the biphenyl mesogens on the diagram of liquid crystal phase would provide a great deal of information on the relation between the mesogen molecular structure and the mesophase structure.

2 Molecular Design

Among many modification methods, the introduction of the bridge between 2 and 2′ positions of the biphenyl group, like fluorene and fluorenone, would drastically change the properties of biphenyl mesogens.

The changes introduced by the substitution of fluorene for a biphenyl skeleton could be summarized as follows.

1 The rotational degree of freedom of the C-C bond between the two phenyl rings is killed by the introduction of the bridge. Thus, the fluorene mesogens are completely flat[4)]. This implies that the delocalization of the electrons would extend to the adjacent aromatic rings and would result in an increase in the polarizability of mesogens, which enhances intermolecular attractive interaction. Thus the smectic phase would be stabilized[5)].

2 The decrease in the axial ratio for the mesogen group, by the introduction of the "outboard" methylene group, however, would decrease the shape anisotropy for the mesogens

and consequently decrease the thermal stability of the smectic phase.

3 The overall shape of the mesogen changes from a linear rod to a banana-like shape, due to the bending of the biphenyl axis with an angle of about 24°. This deformation would also diminish anisotropy and therefore works against the stabilization of the smectic phase.

The replacement of biphenyl with fluorenone would add two more changes.

4 The carbonyl group attached perpendicularly to the biphenyl axis further increases the molecule width. Thus, thermal stability for the smectic phase would be further reduced.

5 The permanent dipole moment is introduced into the molecule by the carbonyl group, which was pointed out by Van der Meer and Vertorgen[6], to induce smectic C phase.

3 History

Several liquid crystalline materials containing

fluorene and fluorenone structures have been reported. Gray and his co-workers[7] synthesized and investigated the 7-alkoxy-2-carboxylic acids and their n-propyl esters which have fluorene or fluorenone structures (1)-(4). Although the fluorene derivatives

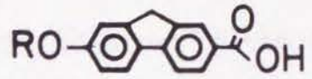
(1)

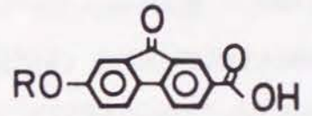
(2)

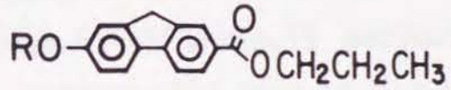
(3)

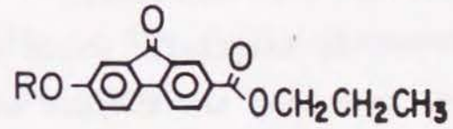
(4)

(1) and (3) showed a smectic (not specified as smectic A, C and others) mesophase in a wide range of temperatures, the fluorenone derivatives (2) and (4) did not show even any kind of mesophase.

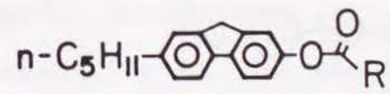
(5)

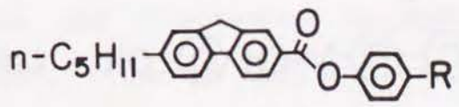
(6)

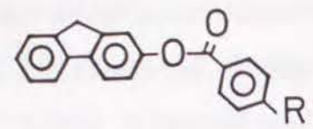

(7)

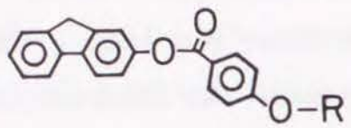

(8)

The fluorene derivatives (5) and (6), and (7) and (8) have been reported by Davidson et al.[8], and Arora et al.[9], respectively. However,in these fluorene derivatives, the smectic C phase was not identified, though the nematic and smectic A phase were observed. Thus concerning fluorene derivatives, no stable smectic C phase has been confirmed.

The liquid crystalline materials, which have a fluorenone structure, have been the subject of very few reports. Gray et al.[10] reported that the fluorenone derivatives (9), (10) showed a stable smectic phase but they did not specify the type of smectic phase in detail.

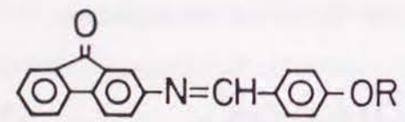

(9)

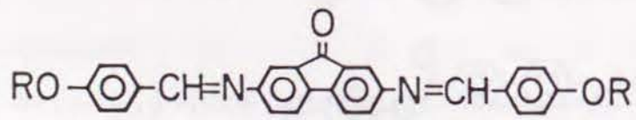

(10)

In these literatures, Gray et al. explained the phase transition behaviors for nematic and smectic phase by using polarizability of the molecules like increased polarizability for conjugation concerning fluorene compounds and molecular shape such as collinearity, planarity and molecular width. However, as described above, smectic phase was not specified like smectic A, C and others and the stability of smectic phase are explained only by lateral or terminal intermolecular cohesion.

This explanation is appropriate for smectic A phase, however, the role of dipole moment and polarizability to the stability of smectic C phase could not be reflected.

Arora et al. described that concerning the fluorene compounds, the coplanarity of the molecule affected the conjugation of the entire molecule, thereby the net polarizability along its major axis and liquid crystalline stability.

Recently Kusabayashi et al.[11] reported the thermal stability of the smectic C phase for the fluorene and fluorenone derivatives (11), (12). (Although, fluorene derivatives (11) did not show

smectic C phase, the stability of smectic C phase for these derivatives was discussed by virtual transition points, which were determined by miscibility tests with other liquid crystalline molecules showing smectic C phase.) They emphasized the importance of the transverse dipole moment, which either resides on the mesogen groups or attaches to the end of them for smectic C phase thermal stability.

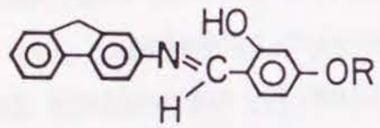

(11)

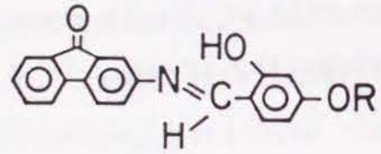

(12)

Thus, the correlation between the mesophase sequence and molecular structural modification of biphenyl, fluorene and fluorenone has not been fully investigated.

To clarify this problem, and together with the desire to develop new ferroelectric liquid crystalline materials having a wide temperature range for the chiral smectic C phase, the author has synthesized fluorene derivatives (13) and fluorenone

derivatives (14) having a chiral group and an alkyl chain with various lengths in a tail of the molecules. By measuring and comparing their mesophase sequence behavior with that for the biphenyl derivatives [12] (15), the structure mesophase correlation for this class of materials is discussed.

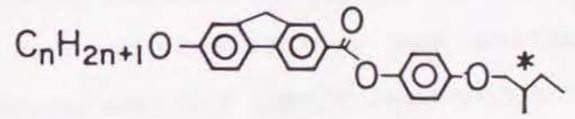

(13)

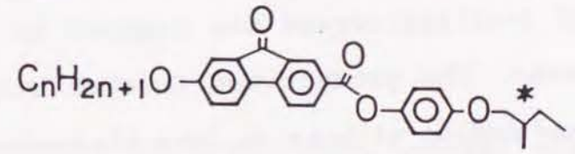

(14)

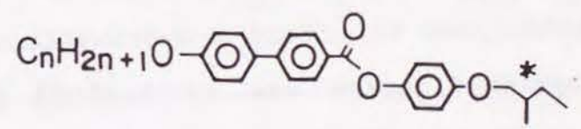

(15)

PART 2 Result and Discussion

1 Syntheses

1-1 4-((S)-2-Methylbutoxy)phenol

(S)-2-Methylbutan-1-ol was reacted with p-toluenesulfonyl chloride in pyridine to afford (S)-2-methylbutyl p-toluenesulfonate[13]. It was reacted with p-hydroquinone. From the obtained mixture, 4-((S)-2-

methylbutoxy)phenol was separated using silica gel column chromatografy.

1-2 Syntheses of Fluorene and Fluorenone Derivatives

Starting materials for fluorene derivatives (15) were synthesized according to the method reported by Gray[7]. The whole scheme is illustrated in Scheme 1. 2-Hydroxyfluorene was synthesized by the 3 step reactions from fluorene. First, fluorene was nitrated [14]. Obtained 2-nitrofluorene was reduced to afford 2-aminofluorene. The product was treated with sulfuric acid and sodium nitrite to form diazonium salt, which was hydrolyzed to afford 2-hydroxyfluorene[15]. 2-Acetyl-7-hydroxyfluorene was synthesized by the following reactions. First, 2-hydroxyfluorene was treated with acetic anhydride to afford 2-acetyloxyfluorene. Then 2-acetyl-7-acetyloxyfluorene was synthesized by Friedel-Crafts reaction of 2-acetyloxyfluorene with acetyl chloride and aluminum chloride [16]. The product was hydrolyzed to afford 2--acetyl-7-hydroxyfluorene[7]. This compound was an important intermediate for the syntheses of fluorene and fluorenone derivatives.

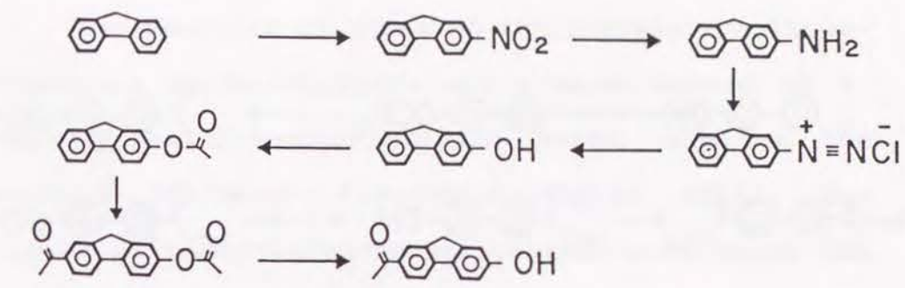

Scheme 1 Syntheses for Fluorene (13), Fluorenone (14) and Biphenyl (15) Derivatives

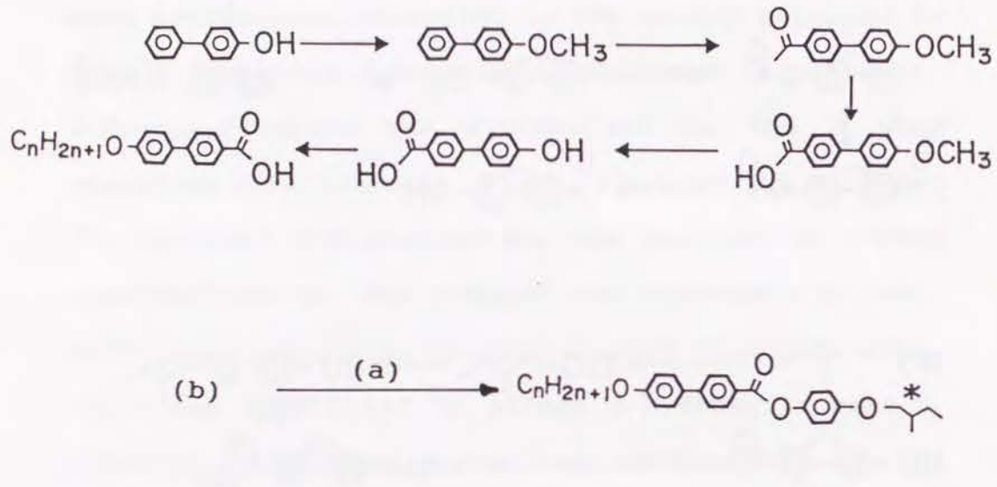

Scheme 2 Syntheses for Fluorene (13), Fluorenone (14) and Biphenyl (15) Derivatives

2-Acetyl-7-alkoxyfluorene was synthesized by the reaction of 2-acetyl-7-hydroxyfluorene and n-alkyl bromide. This product was oxidized by sodium hypobromite.

The reaction mixtures of the 2-acetyl-7-alkoxyfluorenes oxidation contained a small amount of 7--alkoxy-2-fluorenonecarboxylic acids, besides the desired 7-alkoxy-2-fluorenecarboxylic acids. The amount of the fluorenone derivatives were about 15% of the fluorene derivatives.

These mixtures were treated with thionyl chloride, followed by reaction of the cholide with 4-((S)-2-methybutoxy)phenol. The (S)-7-alkoxy-2-fluorenecarboxylic acid 4-(2methylbutoxy)phenyl esters (13) and (S)-7-alkoxy-2-fluorenonecarboxylic acid 4-(2-methylbuthoxy)phenyl esters (14) were separated from the obtained mixture through a column chromatographic technique.

1-3 Syntheses of Biphenyl Derivatives

Although phase transition behaviors for biphenyl compounds (15) are discussed using the data published by Inukai et al.[12] in this chapter, the derivatives

were synthesized[17] for confirmation about detail points. The scheme for the biphenyl compounds (15) was also shown in Scheme 2.

2 Mesophase Transition

The phase transition temperatures for these materials are listed in Tables 1 and 2, and plotted as a function of the alkyl chain length n in Fig. 9 and 10 for molecular structures (13) and (14), respectively. In these figures, the values for the transition temperatures of the biphenyl derivatives (15), published by Inukai and his co-workers [12], having a corresponding terminal alkyl chain, are also indicated with dotted lines.

2-1 Fluorene Derivatives

The overall mesomorphic behavior is qualitatively similar to that of the biphenyl derivatives (15), except for an unidentified smectic phase SmX, which appeared below the smectic C* phase in the cooling process. For the derivatives with n=6 and 8, a thermal hysteresis was observed in the mesophase transition, even with a 5 °C/min cooling and heating

Table 1 Phase transition temperature (T/°C) of (S)-2-alkoxy-7-fluorenecarboxylic acid 4-(2-methylbutoxy)phenyl ester (13)

n	$T_{C\text{-}Sc^*}$ or SA	$T_{Sc^*\text{-}SA}$	$T_{SA\text{-}I}$	$T_{Sc^*\text{-}SX}$ [a]
6	119	[b](87)	208	
8	117	(109)	201	
10	115	137	194	
12	91	144	187	(80)
14	86	143	183	(81)

a C: crystal, Sc*: chiral smectic C, SA: smectic A
SX: smectic X (This smectic phase has not been identified yet)

b ( ): monotropic transition

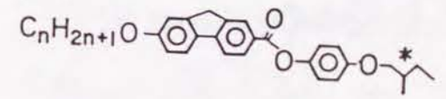

(13)

Table 2 Phase transition temperature (T/°C) of (S)-2-alkoxy-7-fluorenonecarboxylic acid 4-(2-methylbutoxy)phenyl ester (14)

n	T_{C-Sc^*}	$T_{Sc^*-SA \text{ or } I}$	$T_{SA-Ch \text{ or } I}$	T_{Ch-I} [a]
6	100	125	157	165
8	101	140	158	
10	112	157	166	
12	104	158	163	
14	95	147		

a C: crystal, Sc*: chiral smectic C
SA: smectic A, Ch: cholestic

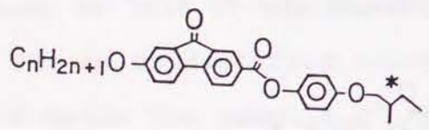

(14)

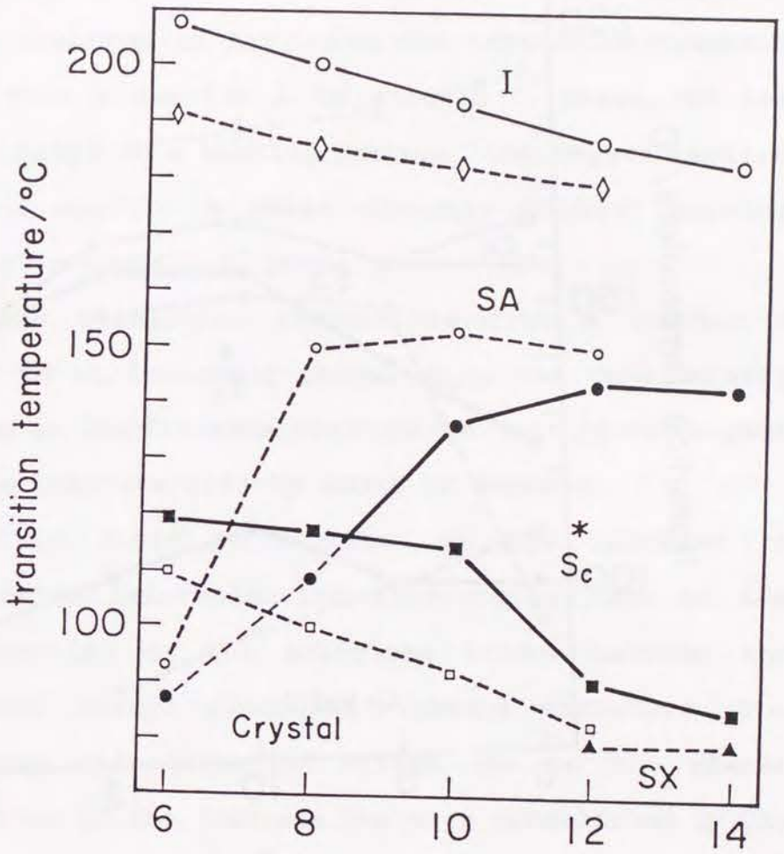

The transition temperature of fluorene series

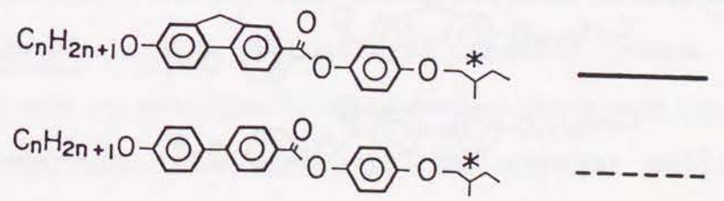

FIGURE 9 The Transition Temperature of Fluorene Series. In this figure, n means the number of carbons of n-alkyl chain in each compound.

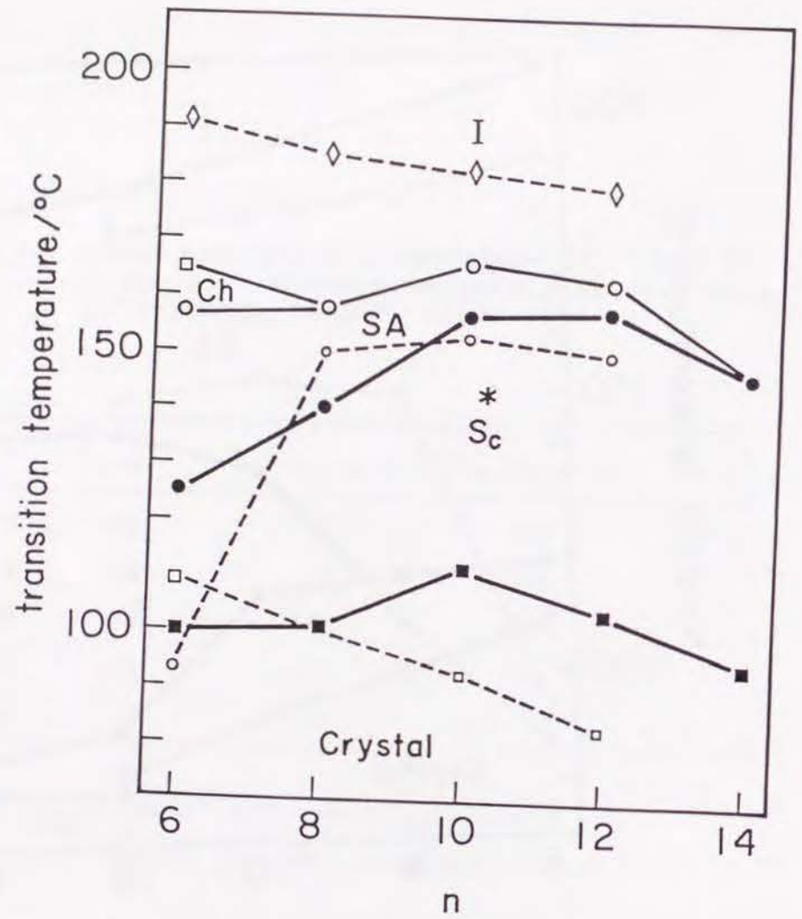

The transition temperature of fluorenone series

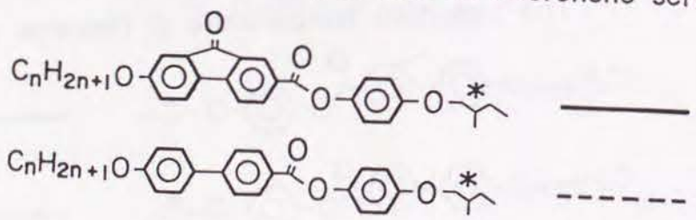

FIGURE 10 The Transition Temperature of Fluorenone Series. In this figure, n means the number of carbons of n-alkyl chain in each compound.

rate. In the cooling process, a transition from a smectic A to smectic C* was observed and crystallization occurred at far below the transition temperature from a smectic A to smectic C* phase. On the other hand, in a heating process, the crystal melted into a smectic A phase directly without passing through a smectic C* phase.

The transition temperature from a smectic A phase to an isotropic phase, T_{SA-I}, was considerably higher in the fluorene derivatives than in the biphenyl derivatives (15) by about 20 degrees.

This could be ascribed to the increase in attractive intermolecular interaction, due to the introduction of the methylene bridge between the adjacent phenyl rings in biphenyl structure. The electron delocalization effect due to the planer structure of the fluorene skeleton established by the introduction of the methylene bridge would increase the polarizability, which leads to the increase of the attractive dispersion force between molecules. This effect would stabilize a smectic phase as pointed out by McMillan[5]. This mechanism seems to be consistent with the fact that the crystal melting

temperature T_M was also higher in the fluorene derivatives (13) than in the biphenyl ones (15) by 40 to 20 degrees, because the higher T_M indicates the stronger cohesion.

The decrease of the T_{SA-I} and T_M with increasing n would be a reflection of the fact that the attractive interaction was diluted by the alkyl chains with low polarizability.

As shown in Fig. 9, the curve of smectic C* to smectic A transition temperature in relation to the number of carbon atoms in the alkyl chain, has maximum both in biphenyl derivatives (15) and fluorene derivatives (13). However, the additional methylene group reduces the thermal stability of the smectic C* phase in the derivatives with n=8 and 10, compared with corresponding biphenyl derivatives (15).

This effect would be explained as follows. The methylene bridge in the fluorene structure makes the molecule planar, which is favorable to mesogenic stability, as indicated by the increasing T_{SA-I}. However, the bridge broadens the molecule and increases the excluded volume. This reduces the thermal

stability of smectic C* phase because the excluded volume effect works to instabilize the smectic C* phase and rather stabilize smectic A phase by packing entropy[6]. Thermal stability of liquid crystals, in which molecules incline in the layer, like smectic C phase decrease rapidly by the increase of molecular width. Because, in these liquid crystal phase, area dominate by molecules increase rapidly with molecular width increasing by the inclination. With larger n, the mesogen modification effect would diminish.

2-2 Fluorenone derivatives

As shown in Fig. 10, mesomorphic behaviors of fluorenone derivatives (14), are rather different from either of the fluorene derivatives (13) and biphenyl derivatives (15) in both smectic A to isotropic phase transitions and smectic C* to smectic A phase transitions.

The T_{SA-I} was remarkably lower than that for the biphenyl derivatives (15). In the fluorenone derivative (14) with n=6, choresteric phase was observed between the smectic A phase and the isotropic phase.

A comparison with the fluorene derivatives (13)

shows that the additional carbonyl group in place of the methylene group of the fluorene derivatives (13) reduces the mesomorphic thermal stability by about 30-50 degrees.

On the other hand, the T_{SC^*-SA} was remarkably higher than that for the fluorene derivatives (13) and even the biphenyl derivatives (15) by 50 degrees at n=6. The temperature range for the smectic A phase narrowed with increasing n. At last, the T_{SA-I} and T_{SC^*-SA} merged at n=14, where the smectic A phase disappeared.

The T_M showed maximum at n=10 in the fluorenone derivatives (14) in contrast to the case in the biphenyl ones (15) where T_M showed minimum at n=12. This difference would be a result of the different packing effect of the alkyl chains between the fluorenone derivatives (14) and biphenyl or fluorene ones (15), (13) with relatively small n. In the derivatives with large n, T_M would be dominated by the terminal alkyl chain and T_M of the three series of derivatives would agree with each other.

The considerable stabilization of a smectic C^* phase in the fluorenone derivatives (14) indicates

that the molecular force, which inclines the molecular axis in a smectic layer, was much enhanced by the introduction of a carbonyl group having a permanent dipolemoment, through the introduction energy mechanism proposed by van der Meer and Vertogen[6].

The transition from the smectic A to smectic C phase is a result of a competition between an attractive induction force and repulsive forces acting between the molecules[6]. The increase in an attractive induction force is suggested by the fact that the T_{SC^*-SA} rose, in spite of the introduction of the bulky carbonyl group, which works to increase repulsive interaction due to the excluded volume effect.

The instabilization of the smectic A phase in fluorenone derivatives (14) would be explained by two factors below. The estimated polarisability of the fluorenone structure is nearly as same as that of the fluorene structure. The carbonyl group, however, will reduce the electron density in the aromatic orbitals. This leads to the decrease of the attractive force which keeps the molecules in smectic layer and thus instabilizes the smectic A phase. Another factor is the decrease of anisotropy of the molecular shape,

because carbonyl group is rather bulky compared with methylene group and molecules rotate freely in liquid crystalline state. The increase of molecular width vividly reduces the thermal stability of smectic A and C phases. Stabilization of smectic C phase in spite of this factor demonstrates the great effect of the dipole moment.

The cholesteric phase was observed in the fluorenone derivative (14) only with short alkyl chain with n=6. This behavior is consistent with the McMillan's theory[5] which predicts that only the first order transition from a smectic A to an isotropic phase is observed for longer molecules. For shorter molecules a transition from a smectic A to a cholesteric phase appears as a first-order phase transition.

2-3 Dominant factor

There are always plural factors for the formation of liquid crystal phases. The stability of smectic A phase is determined by the steric factor and the attractive dispersion force. On the other hand, the stability of smectic C phase is determined

by steric factor and the attractive force between permanent and induced dipole moments. For example, in the case of smectic A phase which fluorene compounds (13) show, the width of the compounds increases and the stability is expected to decrease, compared with that of biphenyl compounds (15). However, the stability increases because of the increased polarizability. In this case, the dominant factor can be said to be attractive dispersion force.

The dominant factors of smectic A, C phases for fluorene and fluorenone compounds are listed in the table below. In smectic C phase, the molecules decline in the layer. So, steric factor for smectic C phase becomes larger than that for smectic A phase. For fluorene compounds, the steric factor reduces the stability of smectic C phase, compensating for the increase of the polarizability. In the case of fluorene compounds, the width of molecules becomes larger than that of fluorene compounds. Nevertheless, the stability of the smectic C phase increase. This fact demonstrates that the attractive force between the permanent and induced dipole moment is extremely strong in the case of fluorene compounds and that the

dipole moment perpendicular to the molecular axis is very effective for the formation of smectic C phase.

The dominant factors for each phase

compound	smectic phase	dominant factor
fluorene deriv.	A	attractive dispersion force
fluorene deriv.	C	steric factor
fluorenone deriv.	A	steric factor
fluorenone deriv.	C	attractive force between permanent and induced dipole moment

PART 3 Conclusions

The thermal stability of smectic C* phase could be increased by an appropriate magnitude of the transverse dipole moment of the carbonyl group for the fluorenone derivatives, even though the mesomorphic stabilities are extremely reduced. Considering

the large difference in the thermal stabilities for the smectic A and C* phases among the fluorene, the fluorenone and the biphenyl derivatives, transverse permanent dipole with appropriate magnitude is a very important factor for the smectic C* phase formation.

The enhancement of the polrizability in the mesogen core is effective to stabilize the smectic A phase.

PART 4 Experiment

Measurements of transition temperatures and microscopic observations of textures of mesophases were made, using an Olympus polarizing microscope in conjunction with a Mettler FP82 heating stage and FP80 control unit and a Daini Seikosha differential scanning calorimeter, model SSC-560s. H-NMR spectra were measured through a JEOL JNM-FX-90 NMR spectrometer for a solution in $CDCl_3$ with tetramethylsilane as the internal standard. IR spectra were recorded on a KBr disc with a JASCO IRA-2 grating infrared spectrometer. Mass spectra were determined with a JEOL DX300 mass spectrometer.

2-Hydroxyfluorene and 2-acetoxyfluorene were

prepared by using the method reported by MacGregor et al[15]. NMR data are described below.

2-hydroxyfluorene

NMR: δ_H (in acetone-d_6) 6.86 (1H, dd, J_{3-1}=3Hz, J_{3-4}=9Hz, H3), 7.03 (1H, d, J_{1-3}=3Hz, H1), 7.09-7.74 (1H, m, H3-H8), 3.80 (2H, s, H9), 8.32 (1H, s, -OH)

2-acetoxyfluorene

NMR: δ_H (in acetone-d_6) 7.09 (1H, dd, J_{3-1}=3Hz, J_{3-4}= 9Hz, H3), 7.20-7.91 (6H, m, H1, H4-8), 3.89 (2H, s, H9), 2.80 (3H, s, $-COCH_3$)

7-Alkoxyfluorene-2-carboxylic acids were prepared by using the method reported by Gray and Ibbotson[7].

2-acetoxy-7-acetylfluorene

NMR: δ_H (in acetone-d_6) 7.17 (1H, dd, J_{3-1}=3Hz, J_{3-4}=9Hz, H3), 7.37 (1H, d, J_{1-3}=3Hz, H1) 7.80-8.20 (4H, m, H4-6, H8) 3.97 (2H, s, H9) 2.60 (3H, s, $-COCH_3$) 2.29 (3H, s, $-OCOCH_3$)

2-acetoxy-7-hydroxyfluorene

NMR: δ_H (in acetone-d_6) 6.91 (1H, dd, J_{6-5}=9Hz, J_{6-8}= 3Hz, H6), 7.09 (1H, d, J_{8-6}=3Hz, H8) 7.69-8.03 (3H, m, H3,4,5) 8.06(1H, s, H1), 8.60 (1H, s, -OH) 3.89(2H,

s, H9) 2.57 (3H, s, $-COCH_3$)

2-acetyl-7-tetradecanoxyfluorene

NMR:(mixture, Integrals could not be identified.)

δ_H (in CDCl3) 0.77-1.94 (m, $-(CH_2)_{12}CH_3$), 2.64 (s, $-C(O)CH_3$), 3.91 (s, H9), 4.03 (t, $-OCH_2$-R), 7.00 (dd, J_{3-4}=9Hz, J_{3-1}=3Hz, fluorene H3), 7.14 (d, J_{1-3}=3H, fluorene H1), 7.68-7.78 (m, fluorene H4, H5), 8.00 (d, J_{6-5}=9Hz, fluorene 6H), 8.11 (s, fluorne H8)

(S)-2-methylbutoxy p-toluenesulfonate was prepared by the following method reported by Dolphin et al[13].

(S)-2-methylbutoxy p-toluenesulfonate

NMR: δ_H (in acetone-d_6) 0.71-1.80 (9H, m, $-CH(CH_3)-CH_2CH_3$), 2.46 (3H, s, toluene-CH_3), 3.89 (2H, d, $J_{OCH2-CH}$=6Hz, $-OCH_2$-R), 7.40-7.89 (4H, m quartet-like, toluene H2, H3, H5, H6)

(S)-4-(2-methylbutoxy) phenol

To a solution of 22.7 g of p-hydroquinone in 100 ml of ethanol, a solution of sodium hydrooxide in 25 ml of water and 50.0 g of (S)-2-methylbutoxy p-toluenesulfonate were added. The solution was heated at 70 °C under reflux condition for four hours. After

cooling to room temperature, the solution was extracted with diethyl ether. The resultant solution was washed with water and treated by hydrochloric acid to be pH1. The organic portion was extracted with toluene and the solvent was evaporated from the solution. (S)-4-(2-Methylbutoxy) phenol (14.4 g (39%)) was separated from the residual mixture by using column chromatography on silica gel. NMR: δ_H (in acetone-d_6) 0.77-1.91 (9H, m, $-CH(CH_3)CH_2CH_3$), 3.70 (2H, dd, -OCH2-R), 6.63-6.82 (4H, m, toluene 2H, 3H, 5H, 6H), 7.79 (1H, s, -OH)

The 7-alkoxy-2-fluorenecarboxylic acids were prepared by the oxidation of 2-acetyl-7-alkoxy-fluorene using sodium hypobromite according to the method reported by Gray and Ibbotson[7]. The obtained products contained a small amount of 7-alkoxy-2-fluorenonecarboxylic acids. The mixed products were used in the next reaction without further purification. (In Chapter 3, more refined methods for the derivatives with (S)-4-(1-methylheptyloxy)phenyl group will be described.)

<u>(S)-7-alkoxy-2-fluorenecarboxylic acid 4-(2-methylbutoxy)phenyl ester (13) and (S)-7-alkoxy-2-fluorenonecarboxylic acid 4-(2-methylbutoxy)phenyl ester (14) (n=12)</u>

A mixuture of 3.30 g of 7-alkoxy-2-fluorenecarboxylic acid containing a small amount of 7-alkoxy-2-fluorenonecarboxylic acid and 25 ml of thionyl chloride was heated at 70 °C for one hour. After evaporating thionyl chloride, 14 ml of dry pyridine was added to the solution. Then, 1.88 g of 4-((S)-2-methylbutoxy)phenol in 7 ml of dry pyridine solution was added and the mixture was warmed at 70 °C for 4 hours. Finally, it was poured into acidic ice water. The brown precipitate was collected. The precipitate was purified by colum chromatography.

From the first fraction, 2.44g of white needles were obtained after three times of recrystallization from the toluene solution, and were identified as (S)-7-dodecyloxy-2-fluorenecarboxylic acid 4-(2-methylbutoxy)phenyl ester ((13),n=12) through NMR, MS and IR spectroscopy.

From the second fraction, 420 mg of yellowish needles were obtained after the same purification

process and were identified as (S)-7-dodecyloxy-2-fluorenonecarboxylic acid 4-(2-methylbutoxy)phenyl ester ((14),n=12) by the same method. The purity of the sample was also checked by HPLC JASCO TWINCLE.

[NMR and IR] The following data for dodecyloxy derivatives are typical of the homologous series as a whole:

For (13), ν_{max} (KBr) 2900, 2850, 1730, 1610, 1510, 1470, 1280, 1250, 1200, 1160, 1100, 840, 770, 740 (cm^{-1}) ; δ_H (in $CDCl_3$) 0.81-1.91 (32H, m, $-(CH_2)_{11}-CH_3$ and $-CH(CH_3)CH_2CH_3$), 3.78 (2H, dd, ArO-CH_2-), 3.87 (2H, s, fluorene-CH_2), 4.03 (2H, t, R-CH_2-O-fluorene), 7.25 6.87 (6H, m, fluorene (1 and 3) H, -OArO- (2,3,5 and 6) H), 7.74 (2H, d, fluorene (4 and 5) H), 8.20 (1H, d, fluorene 6H), 8.28 (1H, s, fluorene 8H)

For (14), ν_{max} (KBr) 2900, 2850, 1730, 1720, 1600, 1510, 1500, 1470, 1300, 1270, 1200, 1140, 1120, 1090, 830, 790, 770, 740 (cm^{-1});δ_H (in $CDCl_3$) 0.88-1.91 (32H, m, $-(CH_2)_{11}CH_3$ and $-CH(CH_3)CH_2CH_3$), 3.78 (2H, dd, ArO-CH_2-), 4.02 (2H, t, R-CH_2O--fluorene), 6.86-7.25 (6H, m, fluorene (1 and 3) H, -OArO- (2, 3, 6 and 5)H), 7.50 (2H, d, fluorene (4 and 5)H), 8.29 (1H, dd, fluorene 6H), 8.38 (1H, s,

fluorene 8H)

[Others]

The data of mass spectroscopy and elemental analysis or exact mass spectroscopy for each derivative are summarized below.

For (13), (n=6) MS m/z 472 (M^+). Anal Calcd for $C_{31}H_{36}O_4$: C, 78.78; H, 7.68 Found: C, 79.14; H, 7.87. Exact mass found M^+ 472.260255, $C_{31}H_{36}O_4$ requires 472.261360, (n=8) MS m/z 500 (M^+). Exact mass found M^+ 500.290785, $C_{33}H_{40}O_4$ requires 500.292660, (n=10) MS m/z 528 (M^+). Exact mass found M^+ 528.323799, $C_{35}H_{44}O_4$ requires 528.323960, (n=12) MS m/z 556 (M^+). Anal Calcd for $C_{37}H_{48}O_4$: C, 79.82; H,8.69 Found: C,79.98 ; H,8.92. Exact mass found M^+ 556.353602, $C_{37}H_{48}O_4$ requires 556.355260, (n=14) MS m/z 584 (M^+).

For (13), (n=6) MS m/z 486 (M^+). Exact mass found M^+ 487.239786, $C_{31}H_{34}O_5$ requires 487.243979, (n=10) MS m/z 542 (M^+). Anal Calcd for $C_{35}H_{42}O_5$: C, 77.46; H, 7.80 Found: C, 77.90; H, 8.03. Exact mass found M^+ 542.307073 , $C_{35}H_{42}O_5$ requires 542.303225, (n=12) MS m/z 570 (M^+). (n=14) MS m/z 598 (M^+). Exact mass found M^+ 598.367188, $C_{39}H_{50}O_5$ requires 598.365825.

REFERENCE

1. K. Takatoh, K. Sunohara and M. Sakamoto, Mol. Cryst. Liq. Cryst., **164**, 167 (1988)
2. J. Billard, Liquid Crystals of One- and Two--Dimensional Orders (edited by W.Helflich and G.Heppke) Springer, Berlin (1980) p.383
3. a) J. W. Goodby and T. M. Leslie, Mol. Cryst. Liq. Cryst., **110**, 175 (1984)
   b) J. W. Goodby and T. M. Leslie, In "Liquid Crystals and Ordered Fluids", Eds. J.F. Johnson and A. C. Griffin, New York, (1984) Vol 4, p1
4. a) D. M. Burns and J. Iball, Nature, **173**, 635 (1954)
   b) G. M. Brown and M. H. Bortner, Acta Cryst., **7**, 139 (1954)
5. W. L. McMillan, Phys. Rev. A4, 1238 (1971)
6. B. W. Van Der Meer and G.Vertogen, J. de Phys., **40**, C3-222 (1979)
7. G. W. Gray and A. Ibbotson, J. Chem. Soc., 3228 (1957)
8. I. R. Davison, D. M. Hall and I. Sage, Mol. Cryst. Liq. Cryst., **129**, 17 (1985)

9. S. L. Arora, B. Ziemnicka and J. W. Doane, Mol. Cryst. Liq. Cryst., **127**, 341 (1985)
10. G. W. Gray, J. B. Hartley, A. Ibbotson and B. Jones, J. Chem. Soc., 4359 (1955)
11. Y. Shimizu and S. Kobayashi, Mol. Cryst. Liq. Cryst., **132**, 221 (1986)
12. (a)T. Inukai, K. Hurukawa, K. Terashima, S. Saitoh, H. Inoue, Proceedins of 10th Liquid Crystal Conference, Tokyo Japan (1984) p.164 (in Japanese)
13. D. Dolphin, Z. Mulijiani, J. Cheng and R. B. Meyer, J. Chem. Phys. 58, (2), 413 (1973)
14. W. E. Kuhn, Org. Synth., 13, 74 (1933)
15. G. W. Gray, J. B. Hartley and A. Ibbotson, J. Chem Soc., 1955, 2686
16. I. R. MacGregor, R. F. Neblett and C. H. Cook, J. Org. Chem., 19, 626 (1954)
17. G. W. Gray, J. B. Hartley and B. Jones, J. Chem. Soc., 1955, 1412

CHAPTER 3 Ferroelectric Liquid Crystal Properties of Fluorene and Fluorenone Derivatives[1)]

PART 1 Introduction

In the previous chapter, the author reported the phase transition behaviors for ferroelectric liquid crystalline materials containing fluorene and fluorenone structures with (S)-2-methylbutoxy group, compared with biphenyl derivatives. In this chapter, the author discussed the relationship between the molecular modifications and the changes in the transition temperatures.

Again, the structural features of fluorene and fluorenone derivatives will be summarized here.

Fluorene derivatives

1. The large polarizability of the mesogen.
2. The outboard methylene group
3. The banana-like shape, due to bending of the biphenyl axis.

Fluorenone derivatives

Two more features are added.

4. The dipole moment, perpendicular to the molecules.

5. The outboard carbonyl group would also decrease the shape anisotropy.

How do features 1-5 act on properties of ferroelectric liquid crystals like the tilt angle and spontaneous polarization?

In this respect, further investigations have been carried out for these materials in the smectic C^* phase. Surface stabilized ferroelectric liquid crystal (SSFLC) cells were constructed. The tilt angle and the spontaneous polarization for these derivatives were measured to clarify the effect of mesogen modification from biphenyl to fluorenone through fluorene.

For this work, the author synthesized the (S)-1-methylheptyl derivatives containing fluorene and fluorenone structures ((16), (17)), together with the derivatives containing the biphenyl structure (18)[2)].

Based on the obtained experimental data, the relationship between the molecular structures and

1) the mesophase behavior
2) the tilt angles
3) the spontaneous polarizations

will be discussed.

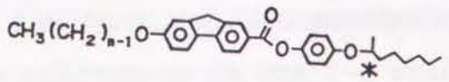

(16)

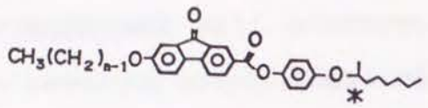

(17)

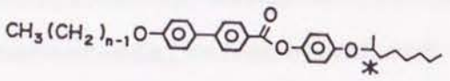

(18)

n = 10, 12, 14

PART 2 Result and Discussion

2-1 Synthesis

2-1-1 Synthesis of 4-((S)-1-Methylheptyloxy)phenol

4-((S)-1-methylheptyloxy)phenol was synthesized by the reaction of 4-((R)-1-methylheptyloxy) p-toluenesulfonate and phenol. The 4-((R)-1-methylheptyl) p-toluenesulfonate was derived from p-toluenesulfonyl chloride and commercially available (R)-1-methylheptanol.

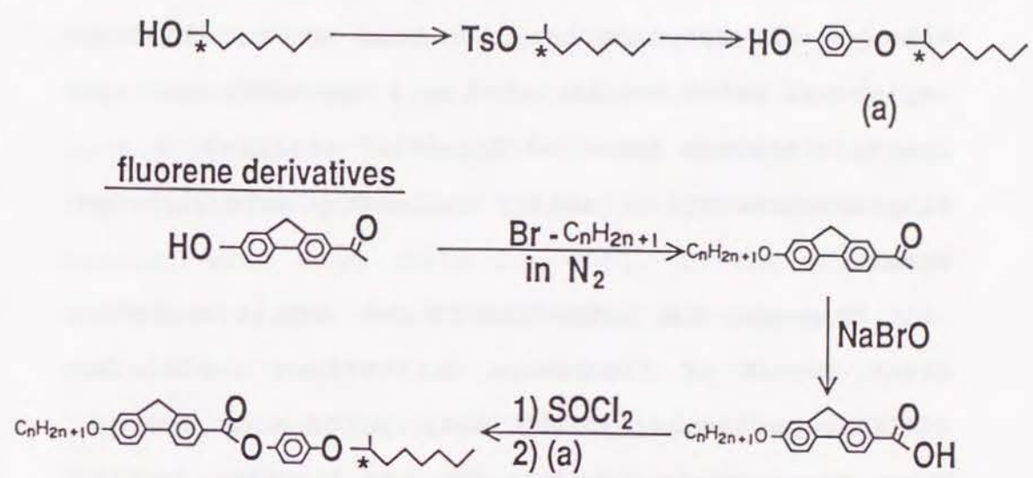

Scheme 3 Syntheses for Fluorene (16) and Fluorenone (17) Derivatives (2)

2-1-2 Oxidation of Metylene Group of Fuorene Structure

As described in the previous chapter, (S)-7-alkoxy-2-fluorenonecarboxylic acid 4-(2-methylbutoxy)phenyl ester was isolated as a byproduct from the reaction mixture intended for (S)-7-alkoxy-2-fluorenecarboxylic acid 4-(2-methylbutoxy)phenyl ester.

However, the author could not obtain a sufficient amount of fluorenone derivatives needed for SSFLC experiments, using this autonomous method. Thus, the synthesis routes for the fluorene derivatives and fluorenone derivatives were investigated separately. It was found that the method shown in the scheme was the most adequate one.

When etherifications of the 2-acetoxy-7-hydroxyfluorene with alkyl bromide were carried out with potassium hydroxide in air, a small amount of 2-acetoxy-7-alkoxyfluorenones was formed with expected 2-acetoxy-7-alkoxyfluorenes, while, in the nitrogen atmosphere, the 2-acetoxy-7-alkoxyfluorenones were not formed. So, it is obvious that the fluorenone derivative was formed by oxidation with oxygen in the

air. From pertinent literature[3], the author learned that the methylene group of the fluorene structure can be oxidized by oxygen with some bases. The author searched for the most adequate condition to support this oxidation reaction. The oxidation of the fluorene derivatives to the fluorenone derivatives was realized with potassium hydroxide in methylethylketone, with high yield (ca 80%). In the authors' experiment, the result depended largely on the solvent species.

Gray et al. oxidized the fluorene compounds to obtain the fluorenone compounds by using chromic acid in acetic acid. The author also tested this reaction. However, the yield of this reaction is low and purification of the product from the reaction mixture is difficult for the formation of black resine. In addition, the industrial usage of chromic acid is difficult for its toxicity. Therefore, the method for the oxidation using basic condition and oxygen in air is considered to be useful.

In other steps, especially in the etherification of 2-alkoxy-7-hydroxyfluorene, fluorene compounds were carefully treated not to be in contact with air

in the solution, especialy in basic solution.

2-1-3 Formation of Fluorene Compounds (16) and Fluorenone Compounds (17)

2-Acetyl-7-alkoxyfluorenes are oxidized by sodium hypobromite to form 2-acetyl-7-fluorene carboxylic acid exclusively. The C-9 methylene group in fluorene structure was not oxidized at all. The acetyl group of 2-acetyl-7-alkoxyfluorenone was also oxidized by the same condition.

The 7-alkoxy-2-fluorenecarboxylic acids were treated by thionyl chloride and reacted with 4-((S)-1-methylheptyloxy)phenol to form (S)-7-alkoxy-2-fluorenecarboxylic acid 4-(1-methylheptyloxy)phenol esters, fluorene compounds (16).

By using the same procedure, the fluorenone compounds (17) were synthesized from the 7-alkoxy-2-fluorenone carboxylic acids. During the last esterification, the author found the formation of byproduct which also shows liquid crystalline behavior. This material will be discussed in detail in chapter 5.

2-1-4 Formations of Biphenyl Compounds (18)

The biphenyl compounds (18) were prepared according to the reported method.[2)]

2-1-5 Optical Purity

The determination of the optical purities of these compounds are very difficult. The author measured specific rotatory power $[\alpha]_D^{20}$ of (S)-4-(1-methylheptyloxy)phenol. The obtained value was 10.82° (c 2.15, $CHCl_3$). During the author's investigation by using Chemical Abstruct Service (1967-1991, Registry Number=73329-06-3), two measured values have been published, 13° (in benzene)[11)] and 11.4° (in $CHCl_3$)[2)]. Especialy, the latter one is almost the same value as the obtained value within experimental error in the same solvent. So, the obtained (S)-4-(1-methylheptyloxy)phenol can be considered to be optically pure. No reaction does not effect the structure $-C^*H(CH_3)-(CH_2)_5CH_3$. Therefore, the obtained optically active liquid crystalline compounds can be considered to be optically pure.

2-2 Transition Temperatures

In Tables 3, 4 and 5, the transition temperatures for the fluorene derivatives (16), fluorenone derivatives (17) and biphenyl derivatives (18)[2], with the (S)-1-methylheptyloxy group, are shown.

In the case of fluorene derivatives, the smectic A phase was stabilized compared with the data for biphenyl derivatives, as in the case of the derivatives with the (S)-2-methylbutoxy group.

The electron delocalization effect, due to the planar structure of the fluorene skeleton, would greatly increase the polarizability, which leads to an increase in the attractive dispersion force between the molecules. This effect would stabilize the smectic A phase[4].

In the (S)-2-methylbutoxy derivatives, the fluorene substitution considerably reduced the thermal stability of the smectic C* phase, compared with the biphenyl derivatives. In the case of the (S)-1-methylheptyloxy derivatives, there was no significant change in T_{SA-SC*}.

In the 2-methylbutoxy derivatives, by substituting the fluorene structure with the fluorenone

Table 3 Phase transition temperature (T/°C) of (S)-2-alkoxy-7-fluorenecarboxylic acid 4-(1-methylheptyloxy)phenyl ester (16)

n	T_{C-SC*}	T_{SC*-SA}	T_{SA-I} [a]
10	87	123	149
12	88	130	146
14	82	127	141

a C:crystal, SC^* :chiral smectic C, SA:smectic A, I:isotropic liquid

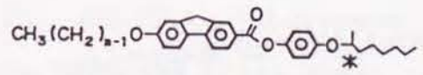

(16)

Table 4 Phase transition temperature (T/°C) of (S)-2-alkoxy-7-fluorenonecarboxylic acid 4-(1-methylheptyloxy)phenyl ester (17)

n	T_{C-SC*}	$T_{SC*-SA\ or\ SC*-I}$	T_{SA-I} [a]
10	81	118	127
12	81	123	126
14	79	115	

a C:crystal, SC^* :chiral smectic C, SA:smectic A, I:isotropic liquid

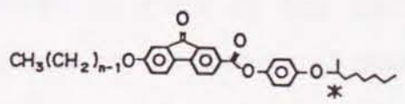

(17)

Table 5 Phase transition temperature (T/°C) of (S)-2-alkoxy-7-biphenylcarboxylic acid 4-(1-methylheptyloxy)phenyl ester (18)

n	T_{C-SC*}	T_{SC*-SA}	T_{SA-I} [a]
10	70	125	143
12	78	127	140
14	82	125	136

a C:crystal, SC^* :chiral smectic C, SA:smectic A, I:isotropic liquid

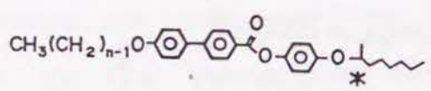

(18)

structure, the thermal stability of the smectic A phase markedly decreased, probably due to the decrease in the shape anisotropy. However, the stabilization of the smectic C^* phase increased. This increasing stability, for a smectic C^* phase, indicates that the molecular force, which inclines the molecular axis in a smectic layer, was much enhanced by the introduction of a carbonyl group having a permanent dipole moment, through the induction energy mechanism proposed by van der Meer and Vertogen[5].

In the case of the (S)-1-methylheptyloxy derivatives, both T_{SA-I} and T_{SC*-SA} decreased, compared with the fluorene derivatives (16). These decreases in the transition temperatures were probably due to the decrease in the shape anisotropy. However, the temperature drop in T_{SC*-SA} was much smaller than that in T_{SA-I}. So, the temperature range for the smectic A phase became quite narrow and T_{SA-I} and T_{SC*-SA} merged at n=14, where the smectic A phase disappeared.

These observations show that, in those fluorenone derivatives (17) with the (S)-1-methylheptyloxy group, the stabilization of the smectic C^* phase by the dipole moment of the carbonyl group perpendicular

to the molecular axis can be admitted.

3 Tilt Angle and Spontaneous Polarization

3-1 Tilt Angle Measurements

The optical tilt angles were measured by the method using ferroelectric liquid crystal cell and polarized microscope[6),7)]. The tilt angle is equal to one half of the microscope stage rotation values, to bring the liquid crystal cell between crossed polarizers into extinction after reversing the applied electric field (15 V). Liquid crystal cells having a 1x1 cm^2 electrode area were used. The alignment was made by coating the glass plate surfaces with polyimide and buffing the surface in one direction. The cell spacing was 2.0 μm, which was obtained by fiber spacers.

In figures 11, 12 and 13, the temperature dependencies of tilt angles for fluorene derivatives (16), fluorenone derivatives (17) and biphenyl derivatives (18)[2)] are shown.

In the case of biphenyl (18) derivatives[2)], the derivatives (n=12, 14) show almost the same values,

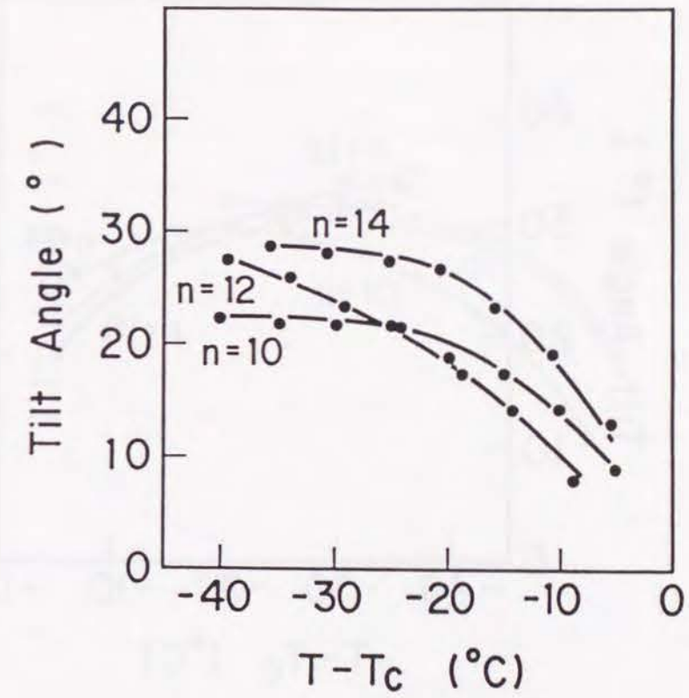

The tilt angle of fluorene series

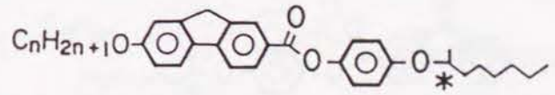

FIGURE 11 Tilt Angle Temperature Dependences for Fluorene Derivatives (16). Tc and n indicate T_{SC^*-SA} and the number of carbon atoms, respectively.

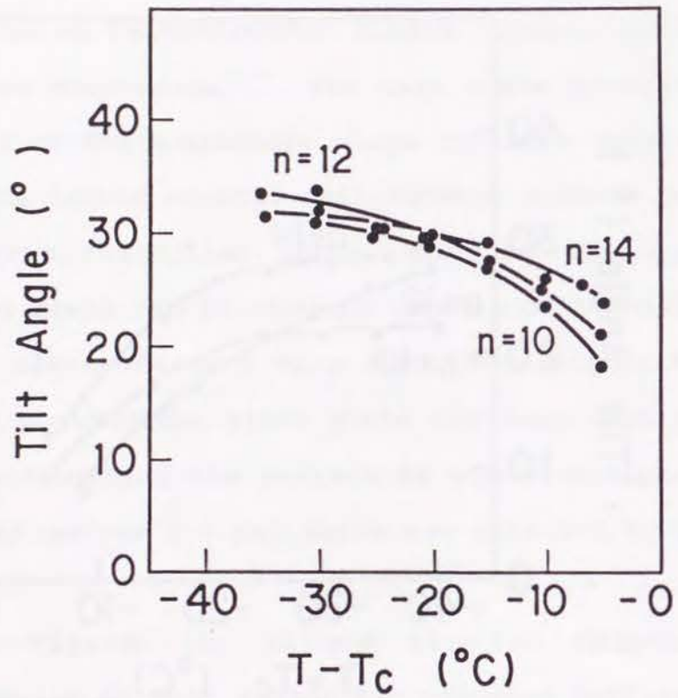

The tilt angle of fluorenone series

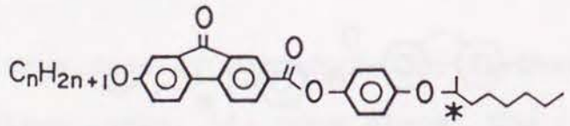

FIGURE 12 Tilt Angle Temperature Dependences for Fluorenone Derivatives (17). Tc and n indicate T_{SC^*-SA} (n=10,12) or T_{SC^*-I} (n=14) and the number of carbon atoms, respectively.

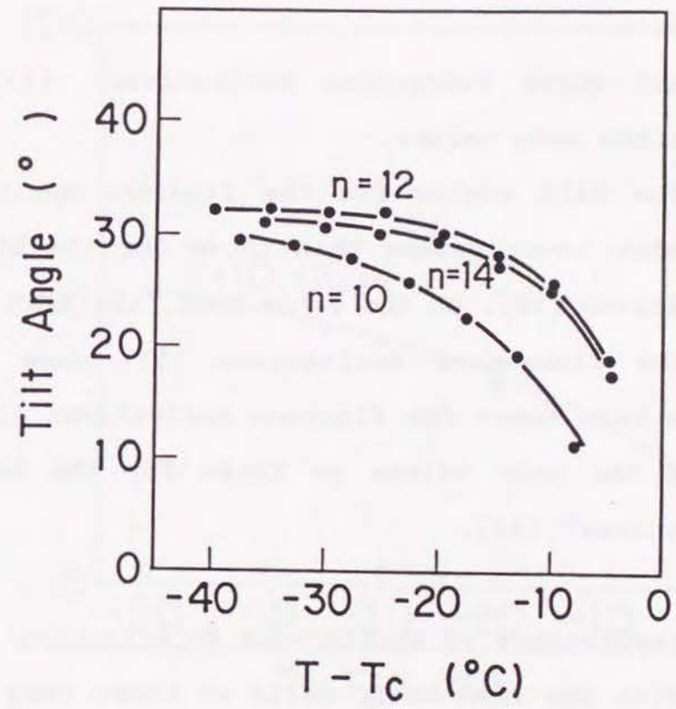

The tilt angle of biphenyl series

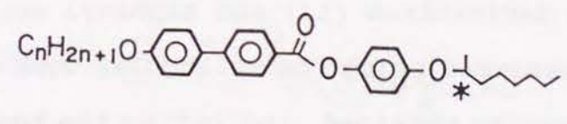

FIGURE 13 Tilt Angle Temperature Dependences for Biphenyle Derivatives (18). Tc and n indicate T_{SC^*-SA} and the number of carbon atoms, respectively.

while the derivative (n=10) shows somewhat lower values.

Regarding the fluorene derivatives (16), the derivatives (n=10, 12) show almost the same values and the derivative (n=14) shows slightly higher values.

All three fluorenone derivatives (17) show almost the same values.

The tilt angles for the fluorene derivatives (16) show lower values than those for the biphenyl derivatives (18). On the other hand, the tilt angles for the fluorenone derivatives (17) show higher values than those for fluorene derivatives (16) and almost the same values as those for the biphenyl derivatives[2] (18).

3-2 Measurements of Spontaneous Polarization

With the same SSFLC cells as those used in the tilt angle measurements, the sizes of the spontaneous polarization for the fluorene derivatives (16), fluorenone derivatives (17) and biphenyl derivatives (18) were measured using the triangular wave method[8].

The results obtained, indicating the temperature

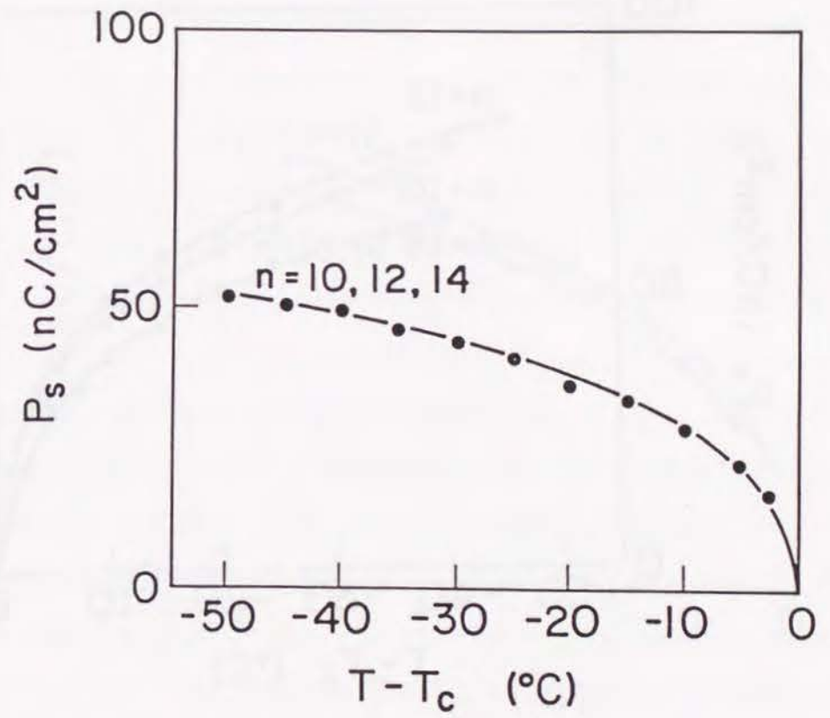

The spontaneous polarization of fluorene series

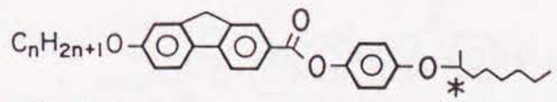

FIGURE 14 Spontaneous Polarization Temperature Dependences for Fluorene Derivatives (16). Tc and n indicate T_{SC^*-SA} and the number of carbon atoms, respectively.

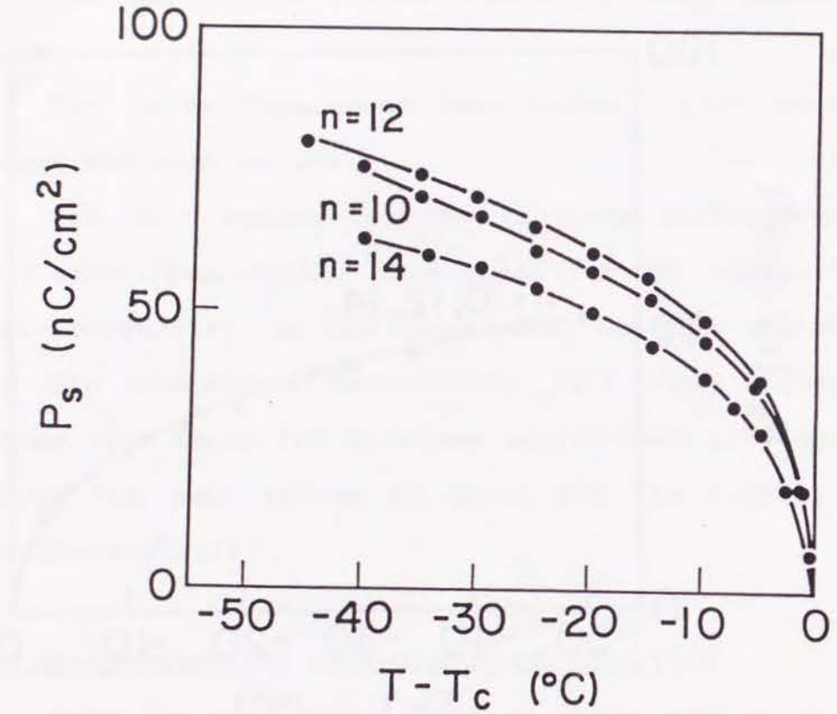

The spontaneous polarization of fluorenone series

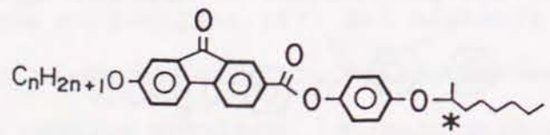

FIGURE 15 Spontaneous Polarization Temperature Dependences for Fluorenone Derivatives (17).Tc and n indicate $T_{SC^*\text{-}SA}$ (n=10, 12) or $T_{SC^*\text{-}I}$ (n=14) and the number of carbon atoms, respectively.

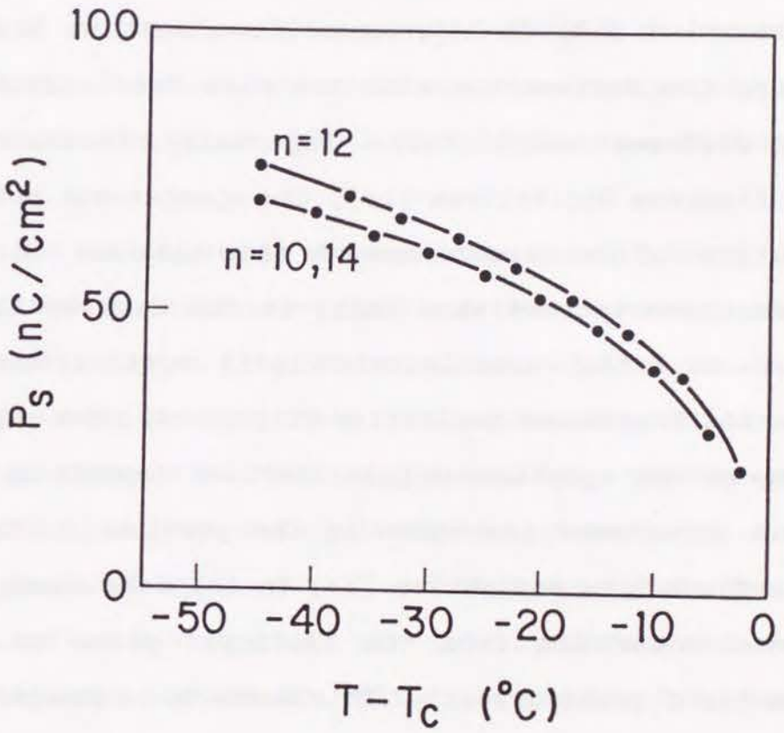

The spontaneous polarization of biphenyl series

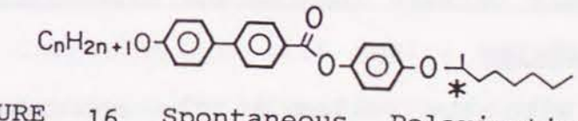

FIGURE 16 Spontaneous Polarization Temperature Dependences for Biphenyl Derivatives (18). Tc and n indicate $T_{SC^*\text{-}SA}$ and the number of carbon atoms, respectively.

dependence of spontaneous polarizations for fluorene derivatives (16), fluorenone derivatives (17) and biphenyl derivatives (18), are shown in Figs. 14, 16 and 17.

In these figures, except for the fluorenone derivative (17) (n=14), there is almost no change among the derivatives with the same core structure and different alkyl chains. Especially, in the case of fluorene derivatives (16), the spontaneous polarizations of the three compounds show the same values. These observations show that, in the case of these three series of ferroelectric liquid crystals, except for the fluorenone derivative (17) (n=14), the magnitude of the spontaneous polarizations depends on the core structures. As shown in the previous section, the fluorenone derivative (17) (n=14) only shows the phase transition from the isotropic phase to the smectic C^* phase directly. This seems to be the reason for the exception.

3-3 Relationship between Spontaneous Polarizations and Tilt Angles

Compared with the values of the spontaneous

polarizations for the biphenyl derivatives (18), those for the fluorene derivatives (16) are rather small.

The reduced tilt angles of fluorene derivatives (16) can be explained by increased volume for addition of outboard methylene group. Because in smectic C phase, in which molecules decline in the layer, increase of molecular width rapidly decrease the tilt angles.

The relationship between the polarizations of the fluorene derivatives (16) and those of the biphenyl derivatives (18) seems to be similar to the relationship between their tilt angles. The relationship between the tilt angle and the spontaneous polarization has been discussed intensively. For example, J.S.Pater et al[6] pointed out that, on a qualitative basis, it is possible to understand the relationship between the tilt angle and the polarization, if one assumes that the increased tilt angle causes a more hindered rotation and thus a larger polarization.

Comparing the tilt angles and the spontaneous polarizations for the fluorenone derivatives (17)

with those for the fluorene derivatives (16), both values for the fluorenone derivatives (17) are greater than those for the fluorene derivatives (16).

The increase in the tilt angle and the spontaneous polarization of fluorenone derivatives (17) could be explained by the introduction of the permanent dipole moment of the carbonyl group.

The induction force, which inclines the molecular axis in the smectic layer, was much enhanced by the introduction of a permanent dipole moment, through the induction energy mechanism [5]. The induction force would make the tilt angle larger and cause a more hindered rotation. This would work to make the spontaneous polarization larger.

The dipole moment, perpendicular to the molecules of ferroelectric liquid crystals, especially the ones near the chiral center, is known to increase the spontaneous polarization directly. However, in the case of the fluorenone molecules, this effect would be negligible, because the distance between the introduced dipole moment and the chiral center is long.

The fluorenone derivative (17) (n=14) shows a

strange behavior. This derivative has a direct phase transition from the isotropic liquid phase to the smectic C^* phase. At this phase transition, as shown in figures 12 and 15, the spontaneous polarization and the tilt angle increase gradually with the decrease in temperature and no discontinuity at T-Tc=0 was clearly observed, as if the phase transition were a second-order one. However, this phenomenon seems to be sometimes observed[9].

PART 3 CONCLUSION

The thermal stabilities for each smectic phase, the tilt angles and the sizes of the spontaneous polarizations are considered to depend on the molecular structure of the central core in the case of fluorene derivatives (16), fluorenone derivatives (17) and biphenyl derivatives (18). In the case of the fluorene derivatives (16), the tilt angles and the sizes of the spontaneous polarizations were decreased, compared with the biphenyl derivatives (18). It can be explained by the increased volume for outboard methylene group.

On the other hand, in the case of the fluorenone

derivatives (17), the tilt angles and the sizes of the spontaneous polarizations were increased, compared with the fluorene derivatives (16). This is due to the induction force, which is introduced by the additional dipole moment perpendicular to the molecule.

Regarding the stabilities of the smectic A phase and the smectic C* phase for the fluorene derivatives (16) and fluorenone derivatives (17), the conclusion reached in the previous chapter was confirmed.

PART 4 Experiment

Measurements of transition temperatures and microscopic observations of the textures of mesophases were made, using an Olympus polarizing microscope in conjunction with a Mettler FP82 heating stage and FP80 control unit and a Seikohdenshi differential scanning calorimeter, model DSC 200. H-NMR spectra were measured through a JEOL JNM-FX-90-NMR spectrometer and JNM-GSX270 NMR spectrometer for a solution in $CDCl_3$, with tetramethylsilane as the internal standard. IR spectra were recorded on a KBr disc with a JASCO Report-100 infrared spectrometer.

Mass spectrometer data were determined with a JEOL DX300 mass spectrometer. The purity value for each sample was checked by HPLC JASCO TWINCLE.

Compound preparation examples are described in the following.

Preparation of 2-acetyl-7-alkoxyfluorenes

The starting materials, 2-acetyl-7--alkoxyfluorenes were synthesized according to the method reported by Gray and Ibboton[10]. However, etherifications were carried out in a nitrogen atmosphere, because the fluorenone compounds were formed as a byproduct on exposure to air in the basic solution.

NMR:(in $CDCl_3$) 0.77-1.94 (27H, m, $-(CH_2)_{12}CH_3$), 2.64 (3H, s, $-C(O)CH_3$), 3.91 (2H, s, H9), 4.03 (2H, t, $-CH_2-R$), 7.00 (1H, dd, J_{3-4}=9H, J_{3-1}=3H, fluorene H3), 7.14 (1H, d, J_{1-3}=3H, fluorene H1), 7.68-7.78 (2H, m, fluorene H4, H5), 8.00 (1H, d, J_{6-5}=9Hz, fluorene 6H), 8.11 (1H, s, fluorne H8)

The 2-acetyl-7-alkoxyfluorenes also show liquid crystalline state, smectic A phase. The phase transition behaviors are described below.

n	T_{Cr-SA}	T_{SA-I}
10	95.0	110.1
12	101.5	107.2
14	105.6	107.4

Preparation of 2-acetyl-7-alkoxyfluorenones (n=14)

The solution of 5.0 g (11.9 mmol) of 2-acetyl-7--tetradecyloxyfluorene and 3.0 g of potassium hydroxide in 150 ml of methylethylketone was heated under reflux for 30 minutes, cooled to room temperature and stirring was continued for 2 hours. The solution was acidified with hydrochloric acid. To collect and wash the precipitate, 3.3 g of yellow crystals were obtained. From the filtrate, 0.9 g of yellow crystals were obtained by column chromatography and recrystallization.

The obtained product was used in the next reaction without further purification. m.p. 106°C, δ_H(in $CDCl_3$,ppm) 0.80-1.83 (27H, m, $-(CH_2)_{12}CH_3$), 2.59 (3H, s, $-COCH_3$), 4.00 (2H, t, fluorenone $-OCH_2-R$), 7.00 (1H, dd, J_{1-3}=3 Hz, J_{3-4}=9 Hz, fluorenone 3H), 7.21

(1H, d, fluorenone 1H), 7.46 (2H, d, fluorenone (4 and 5)H), 8.08 (1H, d, J_{5-6}=9 Hz, fluorenone 6H), 8.12 (1H, s, fluorenone 8H)

Unlike 2-acetyl-7-alkoxyfluorenes, these fluorenone compounds never shows liquid crystalline behavior. (mp.:n=10, 110°C; n=12, 114°C) It is due to the increase of molecular width for the addition of carbonyl group.

Preparation of 7-alkoxy-2-fluorenecarboxylic acids and 7-alkoxy-2-fluorenonecarboxylic acids

2-acetyl-7-alkoxyfluorenes and 2-acetyl-7-alkoxyfluorenones were oxidized by the method reported by Gray and Ibboton[11] to afford 7-alkoxy-2-fluorenecarboxylic acids and 7-alkoxy-2-fluorenone--carboxylic acids, respectively.

Preparation of 4-((S)-1-methylheptyloxy)phenol

4-((R)-1-Methylheptyloxy) p-toluenesulfonate was synthesized according to the method reported by Inukai et al.[2]. NMR (in $CDCl_3$) 0.71-1.77 (16H, m, $-C(CH_3)(CH_2)_5CH_3$), 2.46 (3H, s, toluen-CH_3) 4.60 (1H, m,-O-CH-) 7.28-7.84 (4H, m qualtet-like, toluene

2,3,4,6H)

To a solution of 11.62 g (0.1056 mol) of hydroquinone and 7.10 g (0.1267 mol) of potassium hydroxide in 60 ml of ethanol and 15 ml of water, 30 g (0.11 mmol) of 4-((R)-1-methylheptyloxy) p-toluenesulfonate was added. The solution was heated under reflux for 80 min. After cooling to the room temperature, hydrochloric acid was added to the solution until the pH became 1. The solution was extracted by toluene and the organic layer was washed with water. The solution was dried over potassium carbonate and soluvent was evaporated. Remained oil was purified by using silica gel column chromatography to afford 6.18 g (26 %) of brownish oil. NMR δ_H (in $CDCl_3$) 0.80-1.80 (16H, m,-$C(CH_3)(CH_2)_5CH_3$) 4.20 (1H, m,-CH-) 6.80 (4H, s, phenol 2,3,5,6H) $[\alpha]_D^{20}$=10.8 (c 21, in $CHCl_3$) (11.4° (c 10.1, in $CHCl_3$), lit.[2])

<u>Preparation of (S)-7-alkoxy-2-fluorenecarboxylic acid 4-(1-methylheptyloxy)phenyl ester ((16), n=12)</u>

7-Dodecyloxy-2-fluorenecarboxylic acid (n=12) (2.80 g :7.10 mmol) in 30 ml of thionyl chloride was heated under reflux for one hour. After evaporating

thionyl chloride, 20 ml of dry pyridine was added. Then, 2.21 g (9.95 mmol) of 4-((S)-1-methylheptyloxy)phenol in 10 ml of dry pyridine solution was added and the mixture was warmed at 80 °C for 5 hours. Finally, it was poured into ice water. After acidification, the precipitate was collected. The precipitate was purified by column chromatography. White needles (1.66 g ,2.78 mmol, 39%) were obtained after two recrystallizations from the petroleum ether solution, and were identified as (S)-7-dodecyloxy-2-fluorenecarboxylic acid 4-(1-methylheptyloxy)phenol ester ((16), n=12) through NMR, MS and IR spectroscopy.

The following data for dodecyloxy derivatives are typical of the homologous series as a whole:

ν_{max}(KBr) 2930, 2860, 1725, 1610, 1510, 1470, 1290, 1220, 1200, 1165, 1110, 1070, 830, 770, 740 (cm^{-1}), δ_H (in $CDCl_3$, ppm) 0.86-0.91, 1.28-1.88 (41H, m, $-(CH_2)_{10}CH_3$ and $-C(CH_3)(CH_2)_5CH_3$), 3.94 (2H, s, fluorene-CH_2), 4.04 (2H, t, R-CH_2-O-fluorene), 4.30--4.36 (1H, m, Ar-O-CH(Me)R), 6.91-6.94, 7.10-7.14 (4H, m, -OArO- (2,3,5 and 6)H), 6.98 (1H, dd, J_{5-6}=8.3 Hz, J_{6-8}=2.4 Hz, fluorene 6H), 7.13(1H, d, fluorene 8H),

7.75 (1H, d, fluorene (5 or 4)H), 7.76 (1H, d, fluorene (5 or 4)H), 8.20 (1H, dd, J_{3-4}=7.8Hz, J_{1-3}= 1.0Hz, fluorene 3H), 8.30 (1H, d, fluorene 1H)

Mass spectrum, elemental analysis or exact mass spectrum and specific rotatory power $[\alpha]_D^{20}$ for each derivatives are described below.

(n=10) m/z 570 (M+); exact mass found M+ 570.370056, $C_{38}H_{50}O_4$ requires 570.370911. $[\alpha]_D^{20}$=2.14 (c 10, $CHCl_3$).

(n=12) m/z 598 (M+); exact mass found M+ 598.399835, $C_{40}H_{54}O_4$ requires 598.402211. $[\alpha]_D^{20}$= 2.08 (c 10, $CHCl_3$).

(n=14) m/z 626 (M+); exact mass found M+ 626.431445, $C_{42}H_{58}O_4$ requires 626.433511. $[\alpha]_D^{20}$= 1.98 (c 10, $CHCl_3$).

Preparation of (S)-7-alkoxy-2-fluorenonecarboxylic acid 4-(1-methylheptyloxy)phenyl ester ((17),n=12)

Solution of 1.4 g (3.43 mmol) of 7-dodecyloxy-2-fluorenonecarboxylic acid (n=12) in 30 ml of thionyl chloride was heated under reflux for 1 hour. After evaporating thionyl chloride, 15 ml of dry pyridine was added. Solution of 1.07 g (4.80 mmol) of 4-((S)-1-methylheptyloxy)phenol in 5 ml of dry pyridine solution was added and the mixture was warmed at 80°C for 7 hours. Then, it was poured into ice water.

After acidification, the precipitate was collected. The precipitate was purified by column chromatography. 1.38 g (2.25 mmol, 66 %) of yellow needles were obtained after twice recrystallizations from the petroleum ether solution, and were identified as (S)-7-dodecyloxy-2-fluorenonecarboxylic acid 4-(1-methylheptyloxy)phenyl ester ((17), n=12) through NMR, MS and IR spectroscopy.

The following data for dodecyloxy derivative are typical of the homologous series as a whole:

ν_{max}(KBr) 2940, 2860, 1740, 1720, 1605, 1510, 1495, 1470, 1300, 1270, 1245, 1200, 1145, 1125, 1090, 830, 770, 740 (cm^{-1}), δ_H(in $CDCl_3$, ppm) 0.86-0.91, 1.28-1.86 (39H, m, $-(CH_2)_{10}CH_3$ and $C(CH_3)(CH_2)_5CH_3$), 4.03 (2H, t, $R-CH_2-O$-fluorenone), 4.29-4.36 (1H, m, Ar-O-CH(Me)R), 6.90-6.93, 7.10-7.13 (4H, m, -OArO- (2,3,5 and 6)H), 7.05(1H, dd, J_{5-6}=8.1 Hz, J_{6-8}=2.7 Hz, fluorenone 6H), 7.26 (1H, d, fluorenone 8H), 7.51 (1H, d, fluorenone (5 or 4)H), 7.54 (1H, d, fluorenone (5 or 4)H), 8.31 (1H, dd, J_{3-4}=8.1 Hz, J_{1-3}=2.7 Hz, fluorenone 3H), 8.40 (1H, d, fluorenone 1H)

Mass spectrum, elemental analysis or exact mass spectrum and specific rotatory power $[\alpha]_D^{20}$ for each

derivatives are described below.

(n=10) m/z 584 (M+); Anal Calcd for $C_{38}H_{48}O_5$: C, 78.05 H, 8.27. Found: C, 78.16; H, 8.34. $[\alpha]_D^{20}$= 2.02 (c 10, $CHCl_3$). (n=12) m/z 612 (M+); Anal Calcd for $C_{40}H_{52}O_5$:C, 78.39 H, 8.55. Found: C, 78.73; H, 8.85. $[\alpha]_D^{20}$= 2.28 (c 10, $CHCl_3$). (n=14) m/z 640 (M+); Anal Calcd for $C_{42}H_{56}O_5$: C, 78.71 H, 8.81. Found: C, 78.94; H, 9.08. $[\alpha]_D^{20}$= 2.40 (c 10, $CHCl_3$).

Preparation of (S)-4-alkoxy-4'-biphenylcarboxylic acid 4-(1-methylheptyloxy)phenyl ester (18)

(S)-4-Alkoxy-4'-biphenylcarboxylic acid 4-(1-methylheptyloxy)phenyl esters (18) were prepared according to the method reported previously[2]. The following data for decyloxy derivative are typical of the homologous series as a whole:

ν_{max}(KBr) 2940, 2850, 1730, 1600, 1505, 1470, 1400, 1380, 1290, 1240, 1200, 1090, 1030, 880, 840, 770, 720, 700 (cm^{-1}), δ_H(in $CDCl_3$, ppm) 0.74-1.89 (35H, m,-$(CH_2)_8CH_3$ and -$C(CH_3)(CH_2)_5CH_3$), 4.00 (2H, t, J-$_{-CH2-CH2-}$=6Hz, biphenyl-OCH_2-R) ,4.20-4.46 (1H, m, phenyl-O-CH-), 6.86-7.26 (6H, m, biphenyl H3,H5 and phenyl H2, H3, H5, H6), 7.54-7.74 (4H, m, biphenyl

H2, H6, H2', H6') 8.23 (2H, d, biphenyl H3, H5)

Mass spectrum, and specific rotatory power $[\alpha]_D^{20}$ for each derivatives are described below.(n=10) m/z 559 (M+), $[\alpha]_D^{20}$ 5.27 (c 10, $CHCl_3$). (n=12) m/z 587 (M+), $[\alpha]_D^{20}$ 5.08 (c 10, $CHCl_3$). (n=14) m/z 615 (M+), $[\alpha]_D^{20}$ 3.55 (c 10, $CHCl_3$).

References

1. K. Takatoh and M. Sakamoto, Mol. Cryst. Liq. Cryst 182B, 339 (1990)
2. A part of the biphenyl derivatives have already been reported;
   (a)K. Terashima, M. Ichihashi, M. Kikuchi, K. Furukawa and T. Inukai, Mol. Cryst. Liq. Cryst.,141, 237 (1986)
   (b)T. Inukai, S. Saitoh, H. Inoue, K. Miyazawa, K. Terashima and K. Furukawa, Mol. Cryst. Liq. Cryst., 141, 251 (1986)
3. Y. Spinzak, J. Am. Chem. Soc., 80, 5449 (1958)
4. W. L. McMillan, Phys. Rev. A, 4, 1238 (1971)
5. B. M. van der Meer and G. Vertogen, J. de Phys., 40, C3-222 (1979)

6. J. S. Patel and J. W. Goodby, Mol. Cryst. Liq. Cryst., 144, 117 (1987)
7. B. Otterholm, C. Alstermark, K. Flatischler, A. Dahlgren, S. T. Lagerwall and K. Skarp, Mol. Cryst. Liq. Cryst., 146, 189 (1987)
8. H. Takezoe, K. Kondo, K. Miyasato, S. Abe, T. Tsuchiya, A. Fukuda and E. Kuze, Ferroelectrics, 58, 55 (1984)
9. E. Chin, J. W. Goodby, J. S. Patel, J. M. Geary and T. M. Leslie, Mol. Cryst. Liq. Cryst., 146, 325 (1987)
10 G. W. Gray and A. Ibbotson, J. Chem. Soc., 3228 (1957)
11 K. Okamoto and M. M. Labes, Mol. Cryst. Liq. Cryst. 54, 9 (1979)

CHAPTER 4 Direct Influence of Dipole moment to Spontaneous Polarization

PART 1 Introduction

This chapter reports the properties of two types of ferroelectric liquid crystalline materials, which are structural isomers each other, containing fluorenone structure.

The author has discussed the influences of the substitution of fluorene and fluorenone structures for biphenyl structure, comparing properties like transition temperature, spontaneous polarizations and tilt angles.

The thermal stabilization of the smectic C* phase of fluorenone compounds could be admitted. The reason is that the liquid crystalline molecules would be inclined by the induction force, which is induced by the dipole moment of carbonyl group in fluorenone structure perpendicular to the molecular axis, as pointed by van der Meer and Vertorgen[1]. Furthermore, the tilt angles and spontaneous polarizations of fluorenone compounds are larger than those of fluorene compounds. The larger tilt angles can also be

explained by the molecular inclining through the induction force. It is well known that there is a correlation between tilt angles and spontaneous polarizations[2]. The larger spontaneous polarizations are considered to be ascribed to the larger tilt angles.

In this manner the dipole moment introduced by the carbonyl group, perpendicular to the molecular axis of fluorenone derivatives, greatly influences the properties for ferroelectric liquid crystals.

The shorter distance between dipole moment and chiral center results to larger spontaneous polarization. From that point of view, comparison between spontaneous polarizations of compound (17) and those of compound (19), in which carbonyl group of the fluorenone skeleton is brought closer to the chiral center, is interesting.

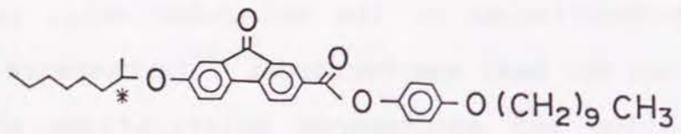

(19)

Author synthesized compound (19) and compared phase transition behaviors, tilt angles and spontaneous polarizations with those for compound (17) (n=10), which is the structural isomer of compound (19).

PART 2 Result and Discussion

2-1 Phase Transition Behavior

Compounds (17) (n=10) and (19) show the following phase transition behaviors.

		81°C		118°C	127°C	
Compound (17)	Cr	———	Sc*	———	Sa	——— ISO
(n=10)		70°C			97°C	
Compound (19)	Cr	———	Sc*	———————		ISO

Compound (17) (n=10), in which (S)-1-methylheptyloxy group was attached to the phenyl group, showed Cr-Sc*-Sa-ISO type phase transition. Compound (19), in which the (S)-1-methylhepthyloxy group was attached to the fluorenone structure, showed Cr-Sc*-ISO type phase transition.

R-(Ar)-COO-(Ar')-R' (a)

Ar,Ar':phenyl, biphenyl, naphthyl groups

R,R' :n-alkyl (alkoxy) or branched alkyl (alkoxy) group

Concerning compound (a), D.Coats[3] pointed out general tendency that compounds, in which branched alkyl group is attached to phenol part (Ar'), shows Sc-Sa transition above smectic C phase. On the other hand, compounds, in which branched alkyl group is attached to carbonyl part (Ar), does not show smectic A phase above smectic C phase.

In the case of fluorenone compounds (17) and (19), compound (17) shows Sc*-Sa transition and compound (19) shows Sc*-ISO transition. These behaviors agree with the general tendency described above.

2-2 Tilt Angle and Spontaneous Polarization

In the case of compound (17), although spontaneous polarizations are larger than those for fluorene derivatives (16), the effect of the carbonyl group dipole moment in fluorenone structure to the increase in the spontaneous polarizations is not clear, because of the long distance between the carbonyl

group and chiral center.

On the other hand , in the case of compound (19), the spontaneous polarization could be influenced directly by the dipole moment of fluorenone structure because the carbonyl group of fluorenone structure is brought closer to the chiral center compared with compound (17).

Spontaneous polarization measurements were carried out using the triangular wave method, which was reported in the previous chapter[4]. Liquid crystal cells, having a 1x1 cm^2 electrode area, were used. The alignment was made by coating the glass plate surface with polyimide and buffing on the surface in one direction. Cell spacing was 2.0 μm which was obtained by fiber spacers.

Figure 17 shows obtained temperature dependencies of spontaneous polarizations for compounds (17) (n=10) and (19). As mentioned above, compound (19) shows direct transition from isotropic liquid to the smectic C^* phase. The spontaneous polarization increases abruptly below the transition temperature between isotropic liquid and smectic C^* phase.

On the other hand, compound (17) (n=10) shows

second-order transition from smectic A phase to smectic C* phase. The spontaneous polarization increases gradually with the decreasing temperature, which is characteristic of second-order transition.

Comparing these spontaneous polarization values, compound (19) shows greater values than those for compound (17) (n=10) immediately below the transition temperature. However, at temperature T-Tc=20 °C, the two curves cross over. Below that temperature, the spontaneous polarizations for compounds (17) (n=10) show greater values than those for compound (19).

Considering the difference between the first-order transition and the second-order transition, it is difficult to compare these values simply. However, it can be recognized that the magnitudes of the spontaneous polarizations for these compounds do not differ greatly from each other.

Figure 18 shows temperature dependencies of the tilt angles for compounds (17) (n=10) and (19). The tilt angles were also measured by the method reported described in the previous chapter, using the same cells which were used in the spontaneous polarization measurements.

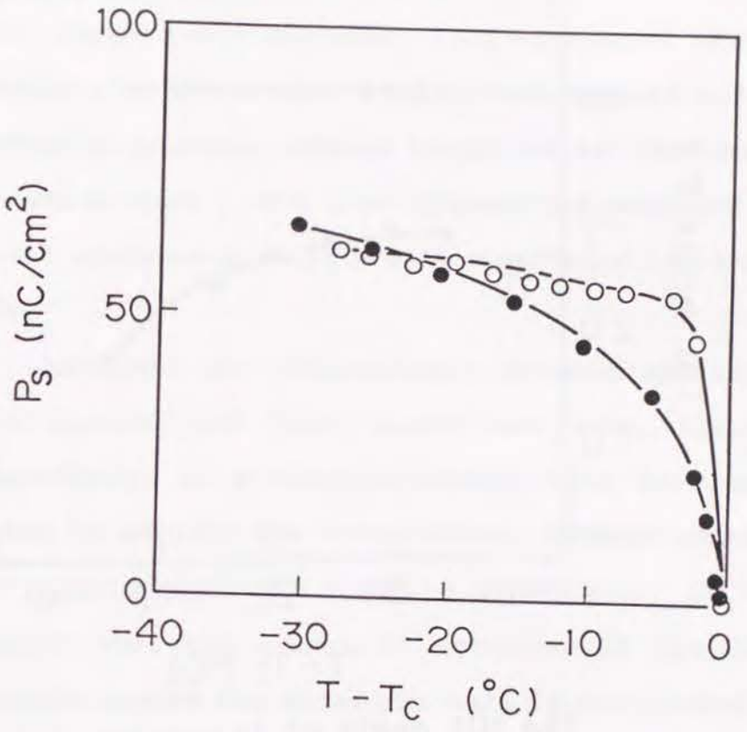

The spontaneous polarization of fluorenone series

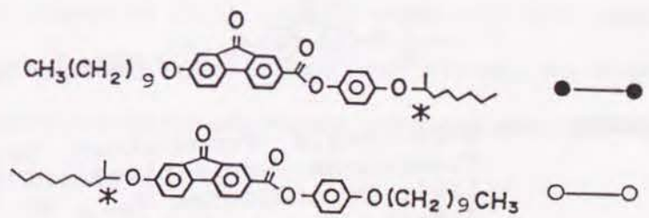

FIGURE 17 Spontaneous Polarization Temperature Dependences for Fluorenone Derivatives (17) (n=10) and (19). Tc indicates T_{SC^*-SA} or T_{SC^*-I}. • and ◦ denote the derivatives (17) (n=10) and (19), respectively.

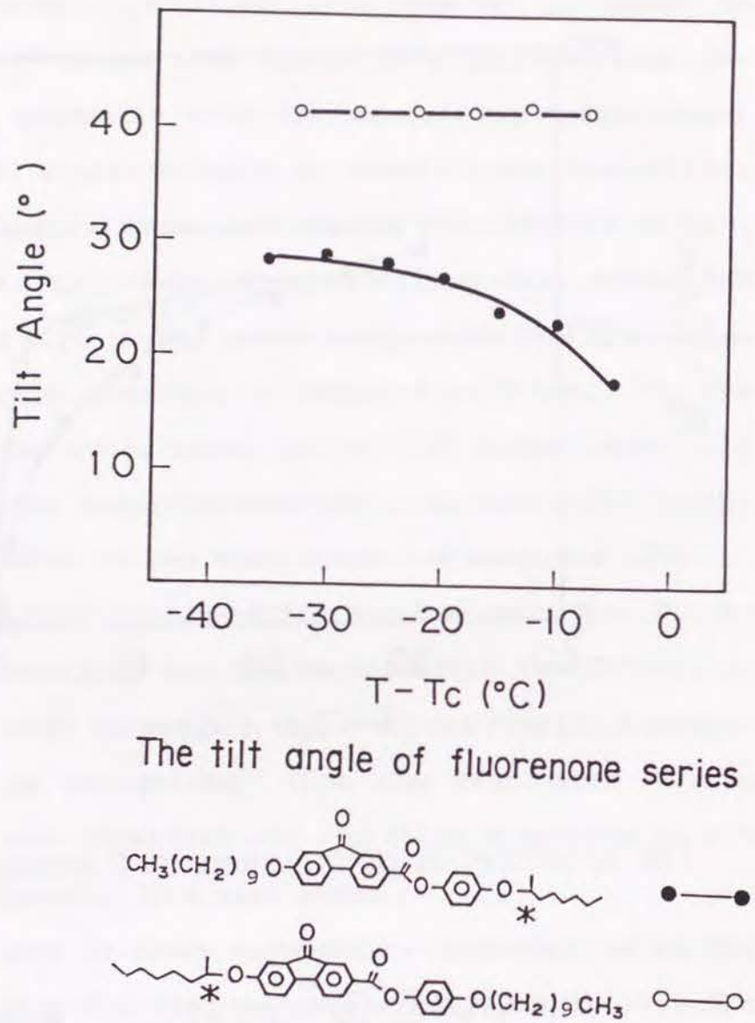

FIGURE 18 Tilt Angle Temperature Dependences for Fluorenone Derivatives (17) (n=10) and (19). Tc indicates T_{SC^*-SA} or T_{SC^*-I}. • and ◦ denote the derivatives (17) (n=10) and (19), respectively.

Similar to the spontaneous polarizations, the tilt angles for compound (19) increase abruptly immediately below the transition temperature and further significant change could not be observed. On the other hand , the tilt angles for compound (17) (n=10) increase gradually with a decrease in temperature.

Although the relationship between spontaneous polarization and tilt angle has been discussed intensively, no systematic theory have been established to explain the correlation between spontaneous polarization and tilt angle. However, if it is assumed that the molecular rotation of the liquid crystals around the molecular axis is restricted with increasing tilt angles, spontaneous polarization are predicted to increase as pointed by J.S.Pater et al[5]. The tilt angles for compound (19) are greater than those for compound (17) (n=10) over all the temperature range. However, as described above, no significant difference between these spontaneous polarizations was found.

This result could be explained as described below.

In the compound (19), the dipole moment of the fluorenone structure is considered to work to reduce the value of spontaneous polarization. As the reason for this, it could be considered that the dipole moment of the ether bond adjacent to the chiral center, which mainly determines the spontaneous polarizations for compound (19), and the carbonyl group of fluorenone structure does not point to the same direction and therefore the dipole moment of the fluorenone structure contributes to a decrease in spontaneous polarization.

PART 3 Conclusion

Concerning the ferroelectric liquid crystalline materials having fluorenone structure, compound (17), in which the chiral center is attached to carbonyl side of the central ester group, shows Sa-Sc* second-order transition. Compound (19), in which the chiral center is attached to the phenol side, shows Sc*-I first-order transition. This tendency was generally observed about liquid crystalline materials, which have ester group between two aromatic groups[3]. The apparent difference of the spontaneous

polarizations between compound (17) and (19) can not be observed, although the tilt angle of (19) is larger than that of (17). Two explanations would be possible. (1) This dipole moment works to reduce spontaneous polarization. (2) Even concerning compound (19), no direct influence of of dipole moment in fluorenone structure to the spontaneous polarization can be observed because of the long distance between the chiral center and the mesogen structure.

PART 4 Experiment

Measurements of transition temperatures and microscopic observations of the textures of mesophases were made, using an Olympus polarizing microscope in conjunction with a Mettler FP82 heating stage and FP80 control unit and a Seikohdenshi differential scanning calorimeter, model DSC 200. H-NMR spectra were measured through a JEOL JNM-FX-90NMR spectrometer and JNM-GSX270 NMR spectrometer for a solution in $CDCl_3$, with tetramethylsilane as the internal standard. IR spectra were recorded on a KBr disc with a JASCO Report-100 infrared spectrometer. Mass spectrometer data were determined with a JEOL DX300 mass

spectrometer. The purity value for each sample was checked by HPLC JASCO TWINCLE.

Preparation of (S)-2-acetyl-7-(1-methylhepthyloxy) fluorenone

(S)-2-Acethyl-7-(1-methylheptyloxy)fluorene was synthesized from (R)-1-methylheptyloxy p-toluene-sulfonate and 2-acethyl-7-hydroxyfluorene, both of which were described in chapter 3. The obtained crude product was used in the next reaction without any purification.

(S)-2-Acethyl-7-(1-methylheptyloxy)fluorenone was synthesized from the obtained (S)-2-acethyl-7-(1-methylheptyloxy)fluorene by using the oxidation reaction, which was described in chapter 3 in detail. mp.51 °C δ_H (in $CDCl_3$, ppm) 0.74-1.80 (16H, m, -$C(CH_3)(CH_2)_5CH_3$), 2.60 (3H, s, -$COCH_3$), 4.34-4.63 (1H, m, fluorenone-OCH-), 7.01 (1H, dd, J_{1-3}=3 Hz, J_{3-4}=9 Hz, fluorenone 3H), 7.24 (1H, d, fluorenone 1H), 7.51 (2H, d, fluorenone (4 and 5)H), 8.11 (1H, d, J_{5-6}=9 Hz, fluorenone 6H), 8.14 (1H, s, 8H)

Preparation of 4-n-decyloxyphenol

4-n-Decyloxyphenol was synthesized from n-decyl bromide and hydroquinone by using the same reaction for 2-acetyl-7-alkoxyfluorene described in chapter 3. δ_H (in $CDCl_3$, ppm) 0.80-1.89 (16H, m, -$(CH_2)_8CH_3$), 3.89 (2H, t, phenyl-OCH_2-), 6.80 (4H, s-like, phenyl (2, 3, 5, 6)H)

Preparation of (S)-7-(1-methylheptyloxy)-2-fluorenone carboxylic acid 4-n-decyloxyphenyl ester (19)

(S)-7-(1-Methylheptyloxy)-2-fluorenonecarboxylic acid 4-n-decyloxyphenyl ester (19) was synthesized by using the same condition as (S)-7-alkoxy-2-fluorenone carboxylic acid 4-(1-methylheptyhoxy)phenyl ester (17), described in chapter 3. ν_{max} (KBr) 2930, 2850, 1720, 1610, 1510, 1470, 1300, 1260, 1250, 1200, 1120, 1100, 1055, 835, 790, 770, 740 (cm^{-1}), δ_H (in $CDCl_3$, ppm) 0.69-1.91 (35H, m, -$(CH_2)_8CH_3$ and -$C(CH_3)(CH_2)_5$-CH_3), 3.94 (2H, t, R-CH2-O-fluorenone), 4.26-4.54 (1H, m, ArO-CH(Me)R), 6.83-7.26 (6H, m, -OArO- (2, 3, 5 and 6)H and fluorenone (6 and 8)H), 7.49 (2H, d, fluorenone (4 and 5)H) 8.26 (1H, dd, J2-3=9Hz, J2-1=2Hz, fluorenone 3H), 8.37 (1H, d, fluorenone 1H) .

Anal. Calcd for C38H48O5: C, 78.05 H, 8.27. Found: C, 78.94 H, 8.35. $[\alpha]_D^{20}$=-13.46° (c 10, $CHCl_3$)

References

1. Van der Meer and G.Vertogen, J.de Phys.40, C3-222(1979).
2. S.Dumrongrattana and C.C.Huang, Phys. Rev. Lett. 56(5) 464 (1986).
3. D.Caotes, Liq. Cryst. 2 (1) 67(1987).
4. H.Takezoe, K.Kondo, K.Miyasato, S.Abe, T.Tsuchiya, A.Fukuda and E.Kuze: Ferroelectrics 58 55 (1984).
7. J.S.Patel and J.W.Goodby: Mol. Cryst. Liq. Cryst. 144 117 (1987).

CHAPTER 5 Formation and Properties of Ferroelectric Liquid Crystalline Compound Containing -C(O)-S-O- Linkage[1)]

PART 1 Introduction

During the synthesis of some fluorenone compounds (17), small amounts of by-products (compound 20) appeared during the step of esterification. After

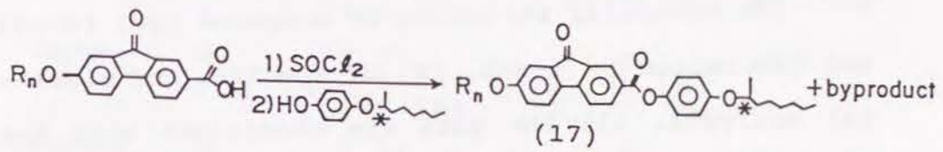

(17)

(n = 10 22% 16%)

isolation and purification, the compound (20) (n=10) was found to show liquid crystal phase over a wide range of temperature under a polarized microscope. For a novel molecular structure of liquid crystalline material and a new reaction, the molecular structure was identified and the properties as ferroelectric liquid crystal was investigated.

PART 2 Results and Discussion

2-1 Formation

The formation of this by-product (compound 20)

has only been confirmed in a few cases. However, in the case of the synthesis of compound (17) (n=10), for example, good amount of compound (20) (n=10) was obtained. The authors discuss this particular case in this chapter. The conditions in this case were given in detail in the experimental section.

2-2 Molecular Structure

The molecular structure of compound (20) (n=10) was determined by ^{1}H-NMR, IR, UV-spectra, and elemental analysis. All the data are consistent with the molecular structure (20) (n=10), shown below.

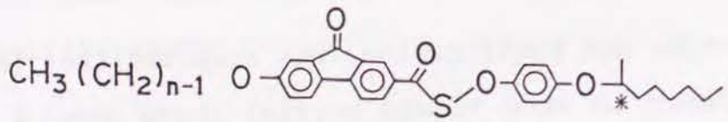

(20)

^{1}H-NMR spectra of compound (17) (n=10) and (20) (n=10) are shown in Table 6. Assignment of each peak was carried out by comparison with the data of other fluorenone derivatives.[2),3)] The chemical shifts and splitting patterns of compounds (17) (n=10) and (20) (n=10) can be assigned reasonably for evry proton.

IR, UV-spectra, and elemental analyses of compound (17) (n=10) and (20) (n=10) are shown in Table 7. IR spectrum of compound (20) (n=10) is very

Table 6 NMR Spectra of Compound (17) (n=10) and Compound (20) (n=10)

Assignment	Chemical Shift δ_H/ppm		Pattern (Integral)
	Compound(17)	Compound(20)	
$-(CH_2)_8CH_3$ and $-C(CH_3)(CH_2)_5CH_3$	1.84-0.86	1.86-0.85	m (35H)
R-CH_2-O-fluorenone	4.03	4.01	t (2H)
Ar-O-CH(Me)R	4.29-4.36	4.32-4.21	m (1H)
-OArO-(2,3,5 and 6)H	6.95-6.89 7.14-7.08	7.14-6.99	m (4H)
fluorenone 6H	7.05 J_{5-6}=8.1Hz J_{6-8}=2.7Hz	6.81 J_{5-6}=8.1Hz J_{6-8}=2.7Hz	dd (1H)
fluorenone 8H	7.26	7.21	d (1H)
fluorenone(5 or 4)H	7.51	7.45	d (1H)
fluorenone(5 or 4)H	7.54	7.47	d (1H)
fluorenone 3H	8.31 J_{3-4}=8.1Hz J_{1-3}=2.7Hz	8.26 J_{3-4}=8.1Hz J_{1-3}=2.7Hz	dd (1H)
fluorenone 1H	8.40	8.33	d (1H)

Table 7 IR and UV Spectra and Elemental Analysis of Compound (17) (n=10) and Compound (20) (n=10)

Compound(17)	IR/cm^{-1} (KBr)	2930, 2860, 1740 (CO), 1720 (CO), 1600, 1510, 1470, 1300, 1270, 1240, 1200, 1090
	λ_{max}/nm (CH_2Cl_2)	435, 339, 325, 283, 252, 231
Compound(20)	IR/cm^{-1} (KBr)	2930, 2860, 1740 (CO), 1720 (CO), 1610, 1490, 1470, 1300, 1260, 1200, 1100
	λ_{max}/nm (CH_2Cl_2)	439, 340, 326, 283, 231
	Elemental Analysis/% (Calcd)	C 74.28 (73.99) H 7.96 (7.84) S 5.44 (5.20)

similar to that of compound (17) (n=10) except that a strong characteristic peak at 1260 cm^{-1} appears and the peak at 1510 cm^{-1} of compound (17) (n=10) disappears. The UV-spectra of the two fluorenone derivatives are essentially same in the region above 260 nm. These spectral properties imply that the main structures making up compound (17) (n=10), such as fluorenone moiety, phenyl and alkyl groups remain in compound (20) (n=10).

Compound (20) (n=10) was purified by triple recrystallization and elemental analysis was carried out at each stage. All analytical results were coincident with the calculated values for the formula $C_{38}H_{48}O_5S$ within experimental error.

Judging from all these results, compound (20) (n=10) was determined to have the chemical formula (20) (n=10).

One possible structure which could explain these data is one with the linkage -C(O)-O-S-. Nevertheless, there seems no possibility for the formation of this structure considering the reaction mechanism.

Compounds containing the -C(O)-S-O- linkage structure have been little reported. The author has

found those compounds mentioned in only 10 papers among the literature published since 1962.

For example, Haas et al[4] reported the formation of $FC(O)SOC(O)CF_3$ by the reaction of fluorocarbonylsulfenic acid chloride (FC(O)SCl) and silver trifluoroacetate($F_3CC(O)OAg$). Schuphan and Casida[5] showed the formation of $(R)_2NC(O)SOCH_2CCl=CH_2$ through [2,3] sigmatropic rearrangement of S-(3-chloroallyl) thiocarbamate sulfoxide ($(R)_2NC(O)S(O)CH_2CCl=CH_2$).

Moon and Oh[6], Islam and Kwart[7] and U. Hildebrand et al[8] reported the formation of a compound containing the -C(O)-S-O- linkage by the reaction of acylsulfenyl chloride derivatives with appropriate alcohol derivatives.

There was no report about a compound with the -C(O)-S-O- linkage which is formed through the reaction of alcohols or phenols with products formed from carboxylic acids and thionyl chloride.

2-3 Phase transition behavior

The phase transition behavior of compound (20) was observed using a polarized microscope in conjunction with a heating stage and a differential scanning

calorimeter.

The phase transition behavior of compound (20) (n=10) is shown below along with that of compound (17) (n=10) , for comparison.

93°C 102°C

Cr——————S_{C^*}——————————————ISO (20)

(n=10)

81°C 118°C 127°C

Cr——————S_{C^*}——————S_A——————ISO (17)

(n=10)

Compound (20) (n=10) shows no tendency to decompose when heated to 200°C in the air. Phase determination was possible because it showed the broken fan texture characteristic of the smectic C phase under a polarized microscope. Miscibility tests were carried out with liquid crystalline materials of which the phase transition behavior was already known. The material exhibits a direct transition from isotropic liquid into chiral smectic C phase. It has higher melting point and lower isotropic liquid - liquid crystal transition temperature than compound (17) (n=10).

The decrease of the mesophase thermal stability, that is the transition temperature from liquid crystal phase to isotropic liquid phase, of compound (20) (n=10) compared with compound (17) (n=10) can be attributed to the fact that the change from -C(O)-O- linkage to -C(O)-S-O- linkage increases the molecular width, decreases the linearity of the molecule and increases the flexibility of the linkage. Especially, disappearance of smectic A phase in the case of compound (20) (n=10) means the decrease of lateral attractive intermolecular interaction because of the factors mentioned above.

After purification by triple recrystallization, and a check of purity using elemental analysis and HPLC each time, the sample is pure enough, but the isotropic phase and chiral smectic C phase coexist in equilibrium over several degrees. The authors experienced this phenomenon in liquid crystalline materials which have a direct transition from isotropic liquid to smectic C phase.[3)]

2-4 Tilt Angle and Spontaneous Polarization

The temperature dependence of tilt angle and

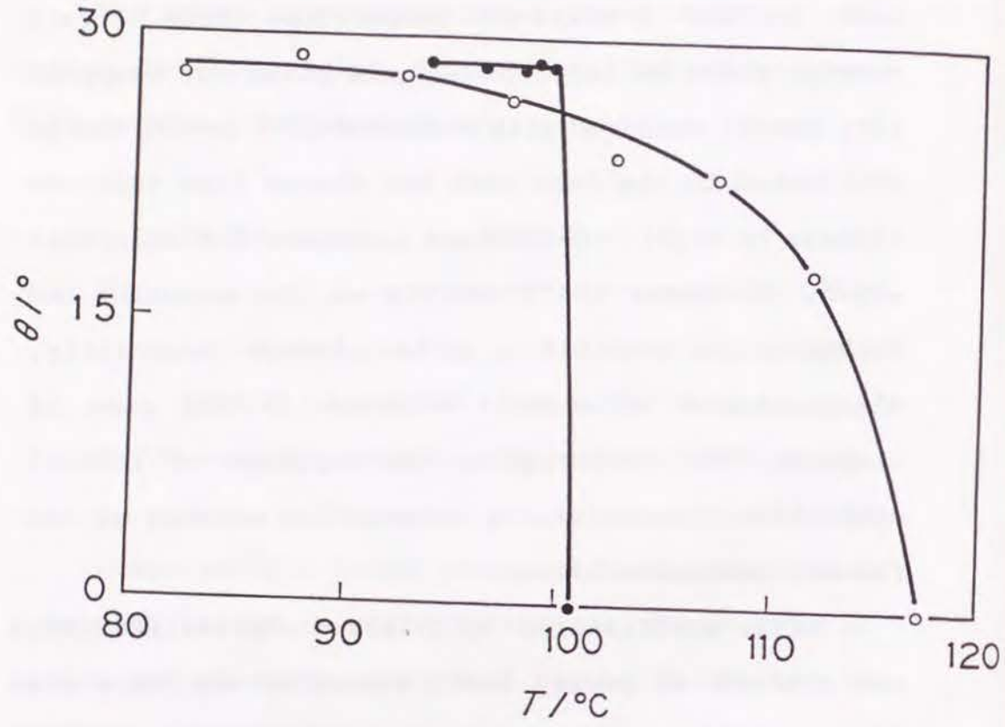

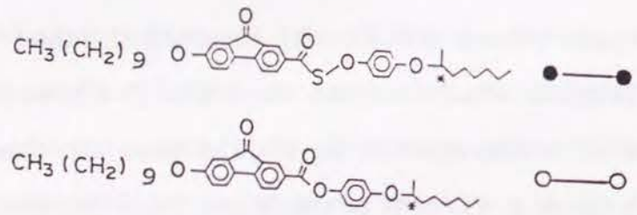

FIGURE 19 Tilt Angle Temperature Dependences of Compound (17) (n=10) and Compound 20 (n=10). • and ◦ denote compound (17) (n=10) and Compound 20 (n=10), respectively.

spontaneous polarization for the compound were measured. These measurements were carried out by the method described in the previous chapter.[3] Liquid crystal cells having a 1x1 cm^2 electrode area were used. Alignment was achieved by coating the glass surfaces with polyimide and buffing the surface in one direction. The cell spacing was 2.0 μm , which was obtained using fiber spacers. In Fig. 19, the temperature dependence of tilt angle for compound (17) (n=10) and compound (20) (n=10) are shown.

Tilt angle of the compound (17) (n=10) increases gradually with decreasing temperature, characteristic of second-order transition. On the other hand, the tilt angle of compound (20) (n=10) increases abruptly to 29 degrees just below the transition from isotropic liquid to chiral smectic C phase, and no significant change was observed. These are characteristic of a first-order transition.

The temperature dependence of spontaneous polarization of compound (17) (n=10) and compound (20) (n=10) are shown in Fig. 20.

Over the whole temperature range, compound (20) (n=10) shows lower spontaneous polarization than

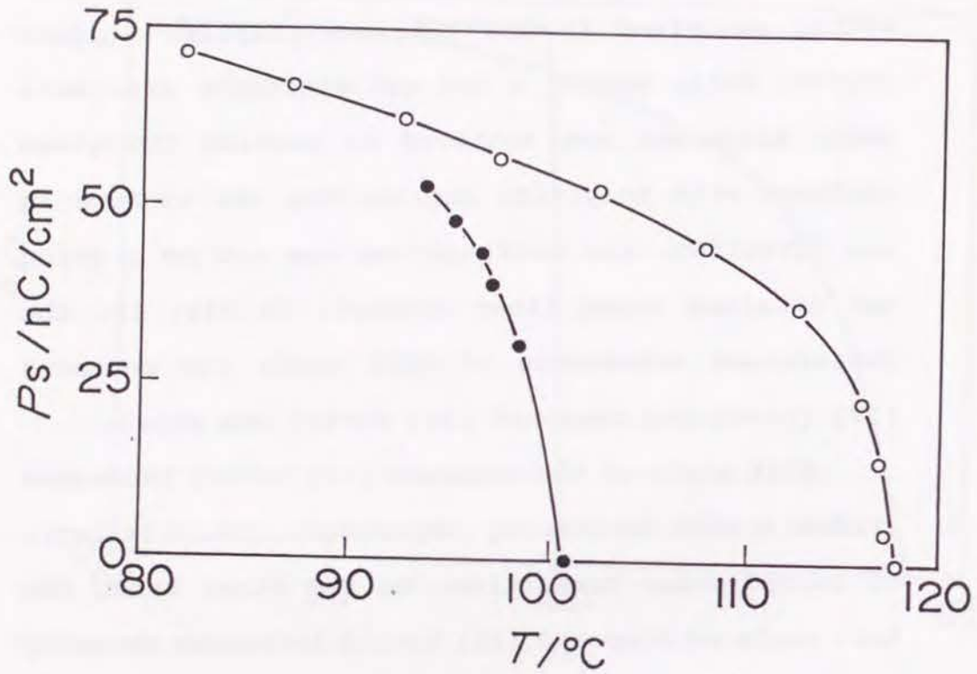

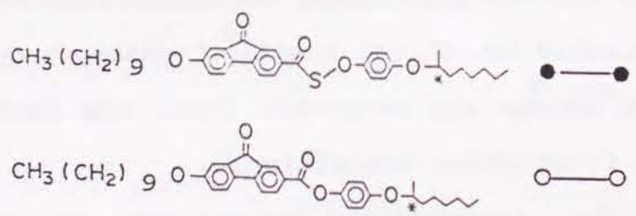

FIGURE 20 Spontaneous Polarization Temperature Dependences of Compound (17) (n=10) and Compound 20 (n=10). • and ◦ denote compound (17) (n=10) and Compound 20 (n=10), respectively.

compound (17) (n=10). Just below the transition temperature, the slope of compound (20) (n=10) is steeper than that of compound (17) (n=10) for the ISO-Sc* type first-order transition. However the spontaneous polarization increases gradually with decreasing temperature, in spite of the first-order transition. This could be ascribed to the fact that, in the case of compound (20) (n=10), the transition between isotropic liquid phase and chiral smectic C phase is ambiguous and both phases co-exist until about 95°C. From these result, it can be said that the change from -C(O)-O- linkage to -C(O)-S-O- linkage does not influence greatly the magnitude of tilt angle and spontaneous polarization.

PART 3 Conclusion

During our investigations on the synthesis of ferroelectric liquid crystal compounds containing fluorenone nucleus, the formation of a novel compound having a -C(O)-S-O- linkage was discovered as a by-product when a derivative of fluorenone carboxylic acid was treated with thionyl chloride and a phenol. This compound also exhibited ferroelectric liquid

crystal properties. The compounds with -C(O)-S-O- linkage are little reported, and this is the first report on a liquid crystalline compound with this linkage. The thermal stability of mesophase, the tilt angle and the spontaneous polarization are reduced by the change from -C(O)-O- linkage to -C(O)-S-O- linkage. These changes can be explained by increased molecular width and flexibility.

PART 4 Experimental

Measurements

Measurements of transition temperature and observations of the microscopic texture of the mesophases were made using an Olympus polarizing microscope in conjunction with a Mettler FP82 heating stage, a FP80 control unit and a Seikohdenshi differential scanning calorimeter, model DSC 200. ^{1}H-NMR spectra were measured using a JEOL JNM-GSX-270 NMR spectrometer for a solution in $CDCl_3$, with tetramethylsilane as the internal standard. IR spectra were recorded on a KBr disc with a JASCO Report-100

infrared spectrometer. The purity of each sample was checked by HPLC JASCO TWINCLE and element analysis.

The Synthesis and Purification of Compound (17) (n=10) and compound (20) (n=10)

7-Decyloxy-2-fluorenonecarboxylic acid (3.00 g, 7.89 mmol) in 35 ml of thionyl chloride was warmed at 70 °C for 2 hours. After evaporating the thionyl chloride, 25 ml of dry pyridine was added. Then 4-((S)-1-methylheptyloxy)phenol (2.21 g, 9.95 mmol) in 10 ml of dry pyridine solution was added and the mixture was warmed at 80 °C for 3 hours. Then it was poured into ice water. After acidification, the precipitate was collected and purified by column chromatography. By recrystallizing the first fraction product from petroleum ether and ethanol solution, 1.02 g (1.75 mmol,22 %) of yellowish needles (17) were obtained. By recrystallizing the second fraction product from petroleum ether and toluene, 0.84 g (1.29 mmol,16 %) of yellowish needles (20) were obtained.

The molecular structures of these compounds were confirmed using ^{1}H-NMR, IR, UV-spectra and elemental

analyses.

References

1.K. Takatoh and M. Sakamoto, Bull. Chem. Soc. Jpn., 64, 2720 (1991)

2. K. Takatoh, K. Sunohara and M. Sakamoto, Mol. Cryst. Liq. Cryst., 164, 167 (1988).

3. K.Takatoh and M.Sakamoto, Mol. Cryst. Liq. Cryst.,182B, 339 (1990).

4. A.Haas, J.Helmbrecht, W.Klug, B.Koch, H.Reinke and J.Sommerhoff, J.Fluorine Chem., 3(3-4), 383 (1973).

5. I.Schuphan and J.E.Casida, Tetrahedron Lett., 1979 (10), 841.

6. S.S.Moon and D.Y.Oh, Taehan Hwahkhoe Chi, 27(2), 157 (1983)

7. N.B.Islam and H.Kwart, J.Chem.Eng.Data., 30(4), 507 (1985).

8. U.Hildebrand, J.Huebner and H.Budzikiewicz, Tetrahedron, 42 (21), 5969 (1986)

CHAPTER 6 Relationship between Fundamental Properties and Behavior as Liquid Crystalline Materials

PART 1 Introduction

For further understanding of the relationship among molecular structures, properties of the compounds and behaviors as liquid crystalline materials containing biphenyl, fluorene and fluorenone compounds, such properties as polarizability, dipole moment and UV-absorption, were measured. Discussions concerning these relationships will be made using the obtained results.

PART 2 Polarizability and Dipole Moment

2-1 Measurement Principle[1)]

The measurement principle will be explained for detailed discussion using obtained results. The dipole moments were calculated from the dielectric constant concentration gradient and dilute solution refractive index, using nonpolar solvent. As nonpolar solvent, tetrachloromethane was used. Measurements for dielectric constant and refractive index were made on solutions, ranging through four kinds of

concentration. The gradients of the graphs for dielectric constant and refractive index were calculated by the least-squares method. Dielectric constants were measured at 10 and 100 Hz. The refractive indices were measured by Abbe refractometer, using D-ray.

Polar molecules have vectorial permanent dipole moment "m", defined by Eq. (1), for inclined electron distribution in the molecule.

$$m=exl \quad (1)$$

(e : magnitude of the charge, l : distance between the centers of positive and negative charges.)

When a molecule is placed in an electric field, electrons shift in the molecule. As a result, a dipole moment is induced in the molecule. This dipole moment is called induced dipole moment m_{ind}. The magnitude of the dipole moment, induced by unit electric field, is called polarizability α.

$$m_{ind}=\alpha \cdot F$$

(F : electric field strength)

Polarizability α is regarded to show the tendency of electrons to move.

Consider a molecule with permanent dipole moment "m" and polarizability "α".

Deformation polarization Pd by induced dipole moment and orientation polarization Po by permanent dipole moment "m" can be defined by the equations below, respectively.

$$Pd=4\pi N\alpha/3$$

$$Po=4\pi Nm^2/9kT$$

(N : Avogadro's number, k : Boltzmann's constant, T : absolute temperature.)

Total polarization P can be defined by the equation (3).

$$P=Pd+Po \quad (3)$$

Molecular orientation by an electric field requires a relatively long time, but electron can be displaced simultaneously. Therefore, when the frequency of the electric field is high enough, polarization is induced only by displacement of electrons, because the molecule cannot be oriented in a short time.

Total polarization P can be expressed by dielectric constant ε, using Clausiusu-Mosotti Eq. (4).

$$M(\varepsilon-1)/\rho(\varepsilon+2)=P \quad (4)$$

(M : molecular weight, ρ : density)

Strictly speaking, this equation can be applicable to the gas phase, although, it can also be used for the dilute solution in a nonpolar solvent.

From the discussion described above, permanent dipole moment "m" can be calculated by measuring total polarizability P and deformation polarizability Pd.

Equations (5) and (6) can hold to a good approximation in the case of a dilute solution of a nonpolar solvent.

$$P_{12}=x_1\times P_1+x_2\times P_2 \quad (5)$$

$$P_{12}=(\varepsilon_{12}-1)\times(x_1\times M_1+x_2\times M_2)/(d_{12}\times(\varepsilon_{12}+2)) \quad (6)$$

(P_{12}, P_1 and P_2 : polarization of solution, nonpolar solvent and solute, x_1 and x_2: molar fractions of nonpolar solvent and solute, M_1 and M_2 : molecular weight of nonpolar solvent and solute, ε_{12} and d_{12}: dielectric constant and density of solution.)

From Eq. (5), it can be understood that P_{12} for a solution changes according to the concentration. To obtain real total polarization of the solute, P_2 was

calculated for several concentrations and extrapolated to an infinite dilution.

In the case of dilute solution, ε_{12} and d_{12} change linearly with the concentration.

$$\varepsilon_{12}=\varepsilon_1+a\times x_2$$

$$d_{12}=d_1+b\times x_2$$

By substituting this ε_{12} and d_{12}, P2∞, the value for P_2 in the infinitely dilute solution, can be represented in Eq. (7).

$$P2\infty=P_1\times\{1+3a/(\varepsilon_1-1)\times(\varepsilon_1+2)-b/d_1\} \quad (7)$$

b can be approximated to zero, because the value is small and the effect can be neglected.

$$P2\infty=P_1\times\{1+3a/(\varepsilon_1-1)\times(\varepsilon_1+2)\} \quad (8)$$

It is known that deformation polarization Pd is almost equal to molecular refraction for visible light.

$$Pd=M/d\times(n^2-1)/(n^2+2) \quad (9)$$

(n : refraction index)

Pd2∞, the deformation polarization of the solute in an infinitely dilute solution, can be shown by Eq.(10), like Eq. (8).

$$Pd2\infty=Pd1\times(1+3c)/(n_1^2-1)\times(n_1^2+2) \quad (10)$$

$$n_{12}^2=n_1^2+c\times x_2$$

(n_{12} and n_1 : refraction index of solution and solvent)

Dipole moment "m" for the solute can be represented by Eq. (11), from Eq. (2), (8) and (10).

$$m=\{9kT\times(P2\infty-Pd2\infty)/4\pi N\}^{1/2} \quad (11)$$

As described above, total polarization, deformation polarization and dipole moment for the polar materials in an infinitely dilute solution can be calculated using the gradient of the graph indicating dielectric constant and refractive index vs. molar fraction for the solution.

2-2 Measurement Method

Detailed conditions for measurement are described below.

Refraction indices were measured by D-ray, using an Abbe Refractometer 2T at 296K. The dielectric constant measurements were carried out, using Hewlett Packard 4192 ALF Impedance Analyzer and Ando Electric Co. Liquid Electrode LE-21 at 296K. The frequencies used were 10 and 100 kHz. As nonpolar solvent, tetrachloromethane was used in both measurements. The concentrations of the solutions were 0.01, 0.025,

0.05 and 0.1 mol/l.

For these measurements, compounds (16) (n=10), (17) (n=10) and (18) (n=10) were used.

2-3 Result and Discussion

Tables 8 and 9 show the dielectric constants and refraction indices for the solutions of biphenyl (18) (n=10), fluorene (16) (n=10) and fluorenone (17) (n=10) compounds for each concentration.

Table 8 Dielectric constants for the solutions of biphenyl (18) (n=10), fluorene (16) (n=10) and fluorenone (17) (n=10) compounds for each concentration

frequency	concentration	(18)	(16)	(17)
10 (kHz)	0.1 (mol/l)	2.300	2.343	2.386
	0.05	2.232	2.271	2.296
	0.025	2.208	2.245	2.244
	0.01	2.198	2.222	2.223
100	0.1	2.295	2.335	2.386
	0.05	2.237	2.269	2.298

0.025	2.205	2.240	2.250
0.01	2.197	2.220	2.225

Table 9 Refraction indices for the solutions of biphenyl (18) (n=10), fluorene (16) (n=10) and fluorenone (17) (n=10) compounds for each concentration

Concentration	(18)	(16)	(17)
0.1 (mol/l)	1.4651	1.4662	1.4661
0.05	1.4618	1.4627	1.4621
0.025	1.4600	1.4608	1.4605
0.01	1.4590	1.4593	1.4592
solvent	1.458		

Tables 10, 11 and 12 show total polarization P, deformation polarization Pd and dipole moment "m" for each compound.

Table 10 Total polarization P for the solutions of biphenyl (18) (n=10), fluorene (16) (n=10) and fluorenone (17) (n=10) compounds (cm^3)

frequency	(18)	(16)	(17)
10 Hz	45.21	48.25	56.49
100	44.80	47.35	55.84

Table 11 Deformation polarization Pd for the solutions of biphenyl (18) (n=10), fluorene (16) (n=10) and fluorenone (17) (n=10) compounds (cm^3)

(18)	(16)	(17)
29.046	29.409	29.425

Table 12 Dipole moment "m" for the solutions of biphenyl (18) (n=10), fluorene (16) (n=10) and fluorenone (17) (n=10) compounds (D)

frequency	(18)	(16)	(17)
10 Hz	0.886	0.957	1.15
100	0.875	0.934	1.13

2-3-1 Deformation Polarization Pd

Deformation polarization Pd is the value which demonstrates charge polarization ease, which is due to the electrons shift in a molecule. The magnitude of this value corresponds to that of polarizability.

To increase this value, two factors should be considered.

1 Introduction of heteroatoms

2 Delocalization of π-electrons in a wide area

The deformation polarizations Pd of biphenyl compounds (18), fluorene compounds (16) and fluorenone (17) compounds increase in that order. However,

the difference between the biphenyl and the fluorene compounds is larger than that between the fluorene and the fluorenone compounds.

The increase in deformation polarization Pd for the substitution of biphenyl structure by fluorene structure can be attributed to delocalization of π-electrons caused by fixation of two phenyl rings in the same plane.

The prospect that the polarizability would be increased for the substitution of biphenyl structure by fluorene structure was one of the main motivations of the molecular design for fluorene compounds and was confirmed by this result.

There is little difference between the deformation polarization of fluorene compound (16) and that of fluorenone compound (17).

Two factors must be considered.

1 Increase in delocalization of π-electrons, because of increasing the π-electron system for addition of carbonyl group.

2 Localization of π-electrons would be increased for the introduction of electron inductive group.

The deformation polarization values for fluorene and fluorenone compounds (16), (17) would not change, because of these contrary factors.

2-3-2 Dipole moment

The dipole moment magnitudes for these compounds increase in order of biphenyl compound (18) (n=10), fluorene compound (16) (n=10) and fluorenone compound (17) (n=10). However, the difference in the magnitude between fluorene and fluorenone compounds is four times larger than that between fluorene and biphenyl compounds.

Measured at 100Hz, the dipole moment for the biphenyl compound (18) (n=10) was 0.875 D and that for fluorene compound (16) (n=10) was 0.934 D. The only difference between these two compounds is that, in the case of fluorene compound (16), a methylene group is introduced and two phenyl rings of biphenyl structure are fixed in the same plane. No polar group with any dipole moment is introduced.

Although the difference between the dipole moments for these two compounds is small, the measured dipole moments for the fluorene compound (16)

(n=10) are larger than those for the biphenyl compound (18) (n=10) at all frequencies and the calculated dipole moments for these compounds show the same tendency (See Chapter 7). Therefore, this difference cannot be regarded as experimental error.

This can be explained by the fact that fluorene, itself, has dipole moment (0.62 D)[2].

The difference in dipole moment magnitude between fluorene compound (16) and fluorenone compounds (17) is large. At 100Hz, the dipole moment for fluorene compound (16) (n=10) is 0.934 D and that for fluorenone compound (17) (n=10) is 1.13 D. The large dipole moment for fluorenone compound (17) is due to carbonyl group in fluorenone structure. This result also coincides with the dipole moment magnitude tendency obtained by molecular orbital calculation.

2-3-3 Total Polarization

Total polarization is considered to be formed from the sum of deformation polarization and dipole moment. Measured at 100kHz, the total polarization for a biphenyl compound (18) (n=10) is 44.80 (cm^3), that for a fluorene compound (16) (n=10) is 47.35

(cm^3) and that for a fluorenone compound (17) (n=10) is 55.47 (cm^3).

From the discussion described above, the difference in total polarization between biphenyl compound (18) and fluorene compound (16) can be ascribed to the difference in deformation polarization, or polarization, between these compounds.

The difference in total polarization between fluorene compound (16) and fluorenone compound (17) is due to the difference in dipole moment between them.

2-4 Effects on Ferroelectric Liquid Crystal Properties

From these measurements, deformation polarizability, dipole moment and total polarization can be calculated concerning biphenyl compound (18) (n=10), fluorene compound (16) (n=10) and fluorenone compound (17) (n=10).

The main features can be summarized as follows.

1 The fluorenone compound has a larger dipole moment, compared to those for biphenyl and fluorene compounds.

2 Fluorene and fluorenone compounds have larger deformation polarization, compared to that for biphenyl compound.

2-4-1 Smectic A Phase Stability

McMillan showed that the attractive dispersion force between molecules stabilizes smectic A phase. The increase in polarizability causes the increase in attractive dispersion force.

Therefore, the increase in deformation polarizability, which was confirmed by these measurement, can explain the stable smectic A phase of the fluorene compound.

On the contrary, although fluorenone compound also shows large deformation polarizability, the smectic A phase stability is low. This can be ascribed to bulky carbonyl group effect in inhibiting the thermal stability for smectic A phase.

2-4-2 Smectic C Phase Stability

From the discussion of Van der Meer and Vertorgen's theory, it can be said that smectic C phase is

stabilized by

1 Large polarizability in mesogen part.

2 Strong dipole moment, perpendicular to the molecular axis.

In the case of fluorene compound, stable smectic C phase would be expected, because of its large deformation polarization. However, the smectic C phase for this compound is not stable. In the case of fluorene compound, increased deformation polarizability has little effect in stabilizing smectic C phase. The thermal stability for the smectic C phase would be reduced by large molecular width of fluorene compound, because, in the smectic C phase case, in which molecules incline in each layer, the thermal stability is easily effected by the molecular width. Decreased tilt angle can be explained by the same reason.

In the case of fluorenone compound, both deformation polarization and dipole moment are large. Therefore, stabilized smectic C phase and large tilt angle can be explained by the result of these measurements.

The increased dipole moment is due to the

carbonyl group in the fluorenone structure. This dipole moment is almost completely perpendicular to the molecular axis and is extremely effective to stabilize smectic C phase, according to the model by Van der Meer and Vertorgen. This dipole moment is also effective to increase tilt angle for the same reason.

PART 3 Electric Spectra

The electronic spectra for fluorene compound (16) (n=10), fluorenone compound (17) (n=10) and biphenyl compound (18) (n=10) were measured using tetrachloromethane as a solvent. Absorption measurements were carried out, using Shimazu UV-VIS recording spectrometer UV-260.

Table 13 Electric spectra

Compound	λmax (nm) (log ε)
Biphenyl (18)	253 (3.97), 302 (4.46)
Fluorene (16)	253 (3.84), 320 (4.51)
Fluorenone (17)	273 (4.58), 309 (3.96), 323 (4.14) 337 (4.16), 430 (3.08)

In Figs. 21, 22 and 23, plots of log ε,(ε : absorption coefficient), vs. wave length are demonstrated. In Table 13, wave lengths for maximum absorptions and log ε in the wave lengths are shown.

The electronic spectra features for these compounds can be summarized, as described below.

1 The electronic spectrum for biphenyl compound (18) is extremely similar to that for fluorene (16) compound.

2 Wave length of maximum absorption $\lambda_{max,}$ in the longest wave length region of fluorene compound (16), is 18 nm longer than that for biphenyl compound (18).

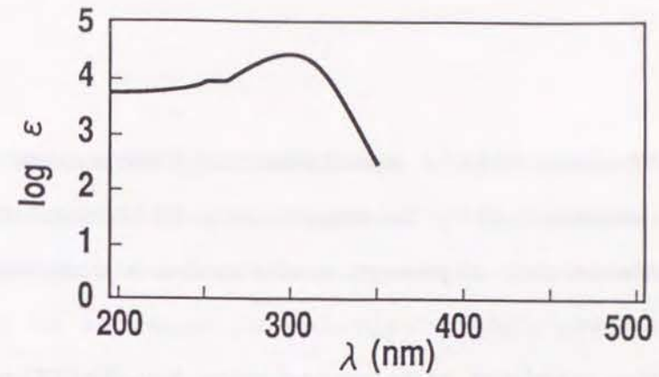

FIGURE 21 UV-VIS Spectrum (in CCl_4) of Biphenyl Compound (18) (n=10).

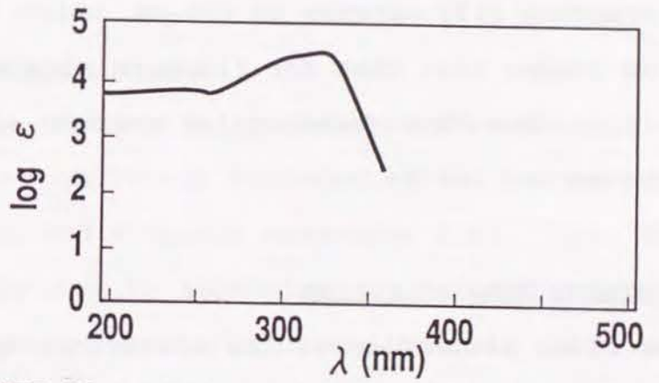

FIGURE 22 UV-VIS Spectrum (in CCl_4) of Fluorene Compound (16) (n=10).

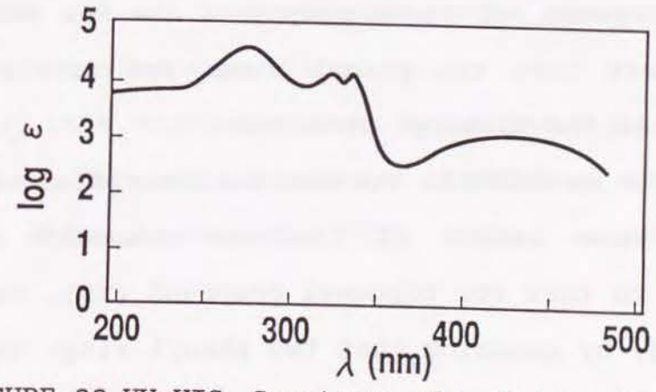

FIGURE 23 UV-VIS Spectrum (in CCl_4) of Fluorenone Compound (17) (n=10).

3 The electronic spectrum for fluorenone compound (17) is completely different from those for biphenyl and fluorene compounds (18), (16).

4 The maximum absorption wave length in the longest wave length region for the fluorenone compound (17) extends to 430 nm, which is 110 nm longer than that for fluorene compound (16). The edge of absorption spectrum extends to around 500 nm.

3-1 Electron Delocalization

The close similarity of the electronic spectra for biphenyl and fluorene compounds (18), (16) reflects the fact that the structures, especially π-electron system, of these compounds are not different, expect that two phenyl rings are twisted or vibrated in the biphenyl structure.

The 18 nm shift in the maximum absorption of the longest wave length of fluorene compound (16), compared to that for biphenyl compound (18), can be explained, by assuming that two phenyl rings in the biphenyl structure are fixed in one plane and π-

electrons are delocalized over a wide area, because this absorption can be ascribed to π-electron system in biphenyl and fluorene structure. This phenomenon implies an increase in polarizability for the fluorene compound and can be related to the smectic A phase stabilization of this compound.

3-2 Dipole moment

The electronic spectrum of fluorenone compound (17) is completely different from the spectra for biphenyl and fluorene compounds (18), (16). This is not only due to expansion of π-electron system by introducing carbonyl group, but is also due to intramolecular charge transfer by introduction of oxygen with high electronegativity. The broad absorption in 430 nm is considered to be intramolecular charge transfer absorption.

By this charge transfer, molecular dipole moment appears. This dipole moment stabilizes smectic C phase and enlarges the tilt angle, as discussed above.

References

1 (a) Y. Morino and I. Miyagawa, In "Soukyokushi Nou ritsu, (Kagaku no Ryouiki Zoukangou)", Nankou-dou (1953) p.5

(b) S. Kobo and Y. Kurita, In "Soukyokushi Moment, (Jikken Kagaku Kouza 3)", Maruzen (1957) p.23

2 V. Baliah and M. K. Pillay, Indian J. Chem. 9, 563 (1971)

CHAPTER 7 Molecular Orbital Calculation

PART 1 Introduction

For further understanding of the behavior of liquid crystalline compounds containing biphenyl, fluorene and fluorenone structures discussed above, molecular orbital calculations were carried out. The program MOPAC was used for this purpose. AM1 semi-empirical Hamiltonian was adopted among Hamiltonians which could be used on MOPAC.

The purpose for this calculation is to explain the relationship among three factors.

1 Features of molecular structures in mesogen part.

2 Properties of compounds, such as the stablest conformation, polarizability and dipole moment.

3 Behavior for liquid crystalline materials.

Therefore, it is justifiable to replace alkyl groups in both ends by methyl group in these calculations. The model compounds can be illustrated like (21), (22) and (23).

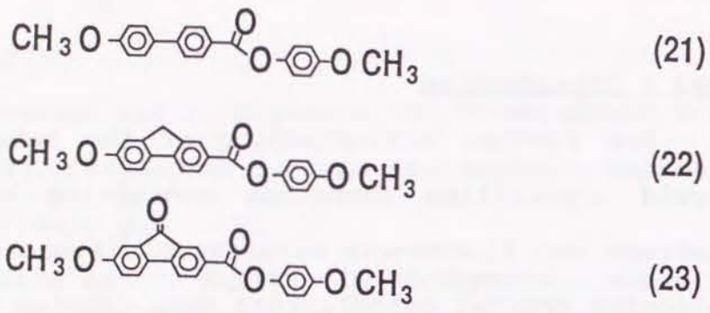

(21)

(22)

(23)

The stablest conformation was determined for each compound. Charge distribution, dipole moment and polarizability were calculated for each determined conformation.

Properties for these compounds and behaviors for the liquid crystalline materials with the same mesogens will be explained, using the obtained results.

PART 2 Stablest Conformations

The stablest conformations for model compounds with structural formulae (21),(22) and (23) are demonstrated in Figs. 24, 25 and 26. Each circle size represents the magnitude of charge on the atom. Shaded part indicates negative charge.

Features described below can be expected by each

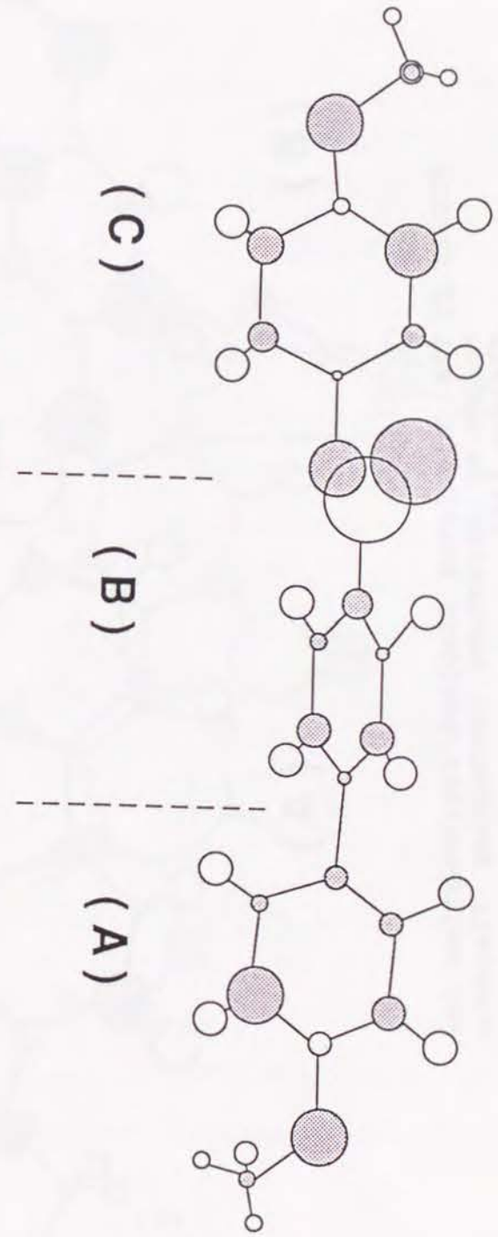

FIGURE 24 The Calculated Stablest Conformation for Molecular Structure Containing Biphenyl Skelton (21)

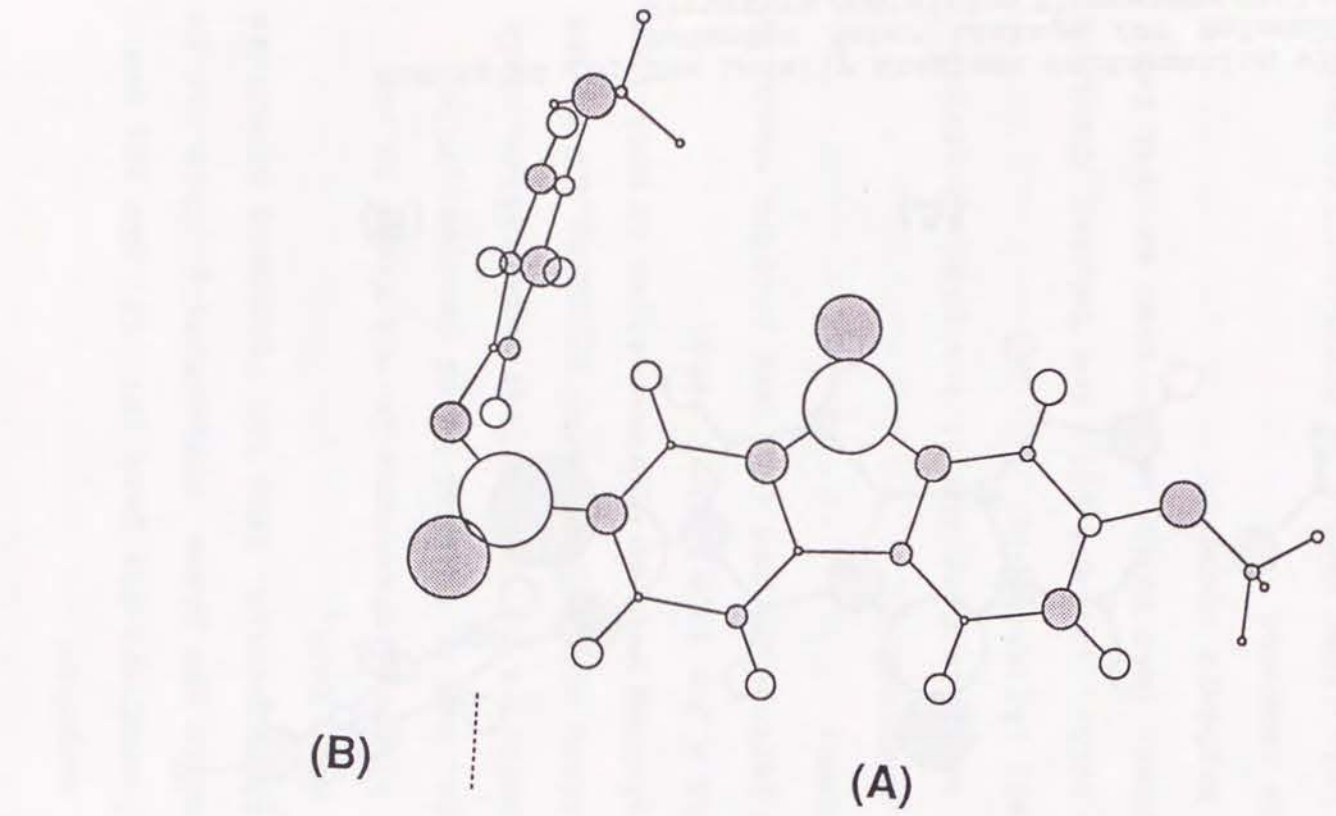

FIGURE 26 (a) The Calculated Stablest Conformation for Molecular Structure Containing Fluorenone Skelton (23)

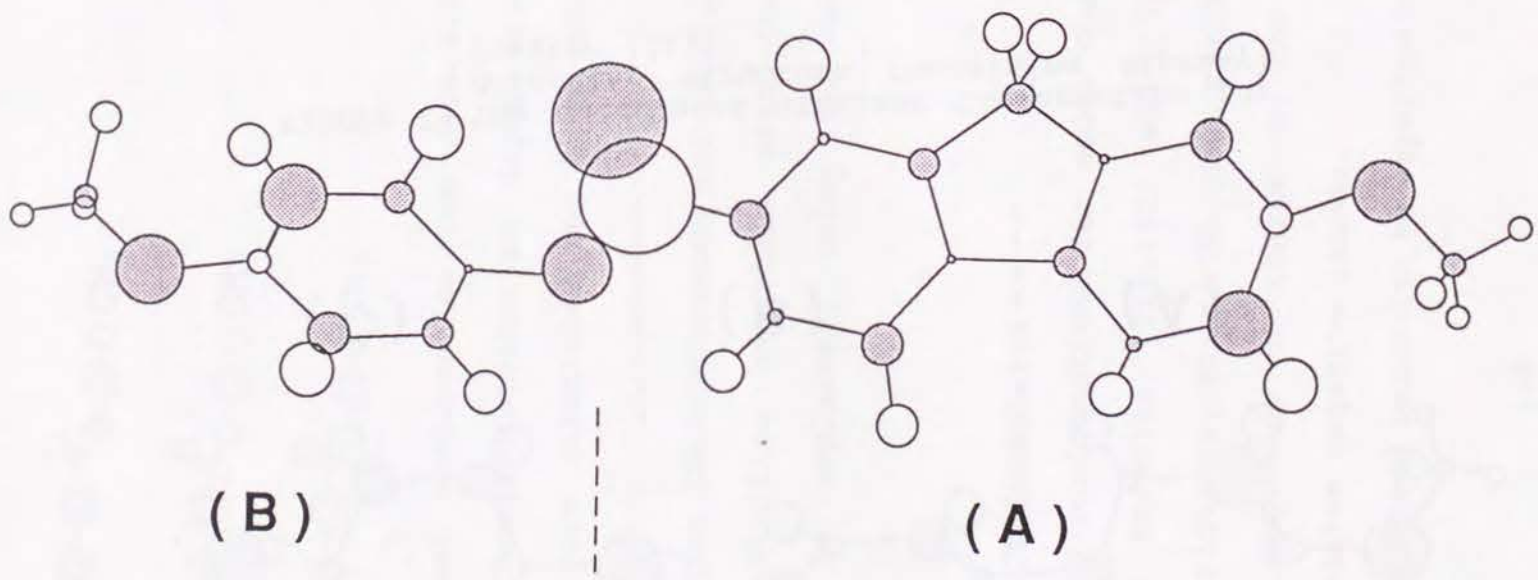

FIGURE 25 The Calculated Stablest Conformation for Molecular Structure Containing Fluorene Skelton (22)

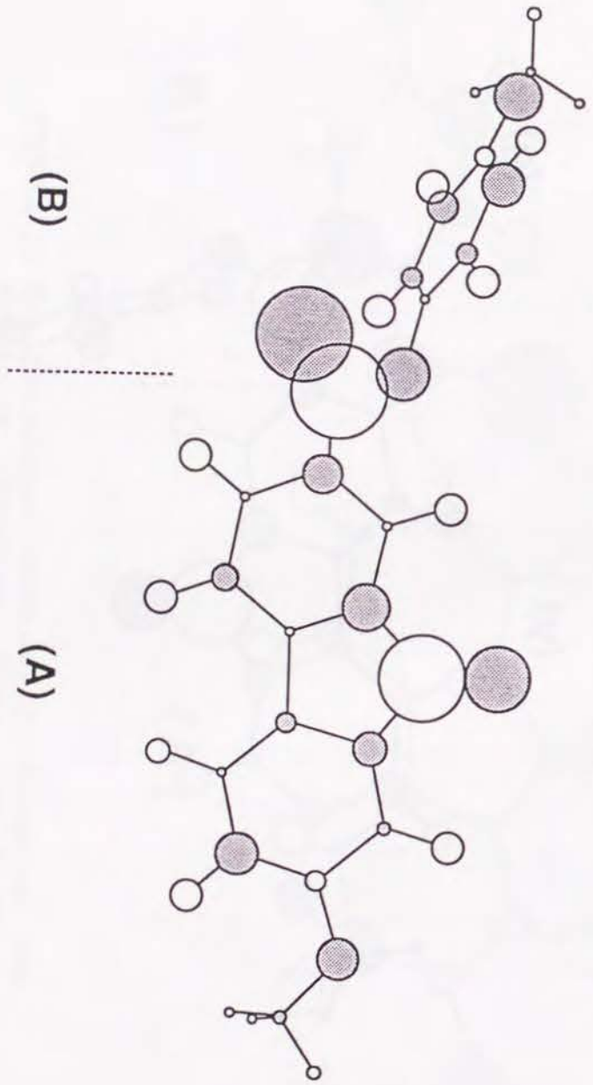

FIGURE 26 (b) The Locally Stablest Conformation with Extended Ester Linkage for Molecular Structure containing Fluorenone Skelton (23)

figure.

1 Biphenyl compound

1 Conformations for part (A), (B) and (C) are fixed in one plane, respectively. This can be easily expected, from the resonance structure for each part.

2 The biphenyl structure is not fixed in one plane, but is twisted by 40 degrees. This corresponds to the initial expectation. This twisting can be considered to occur due to the repulsions between hydrogen atoms in positions 2 and 6 for each phenyl ring.

3 Two parts, (B) and (C), are twisted about 52 degrees.

2 Fluorene compound

1 The molecule consists of two planar structures, (A) and (B).

2 Two parts, (A) and (B), are twisted about 52 degrees. This value is the same as that for the biphenyl compound.

3 Fluorenone compound

The calculated result is completely different from that for biphenyl and fluorene struc-

tures. The ester linkage is largely bent, as shown in Fig. 26 (a). However, in liquid crystalline state, this bent structure is impossible, because of the demand for structural linearity in the liquid crystalline state. Therefore, the energy for the conformation with the extended ester linkage was calculated by fixing the linkage structure to be linear and optimizing locally. The conformation and charge distribution is demonstrated in Fig. 26 (b). The calculated heat of formation for the fully optimized conformation (Fig. 26 (a)) is -96.24 kcal/mol. On the other hand, the heat of formation for the locally optimized conformation with the extended ester linkage is -95.86 kcal/mol. The difference is only 0.38 kcal/mol. Therefore, it seems to be reasonable to adopt the local optimized conformation (Fig. 26 (b)) with the extended ester linkage for further discussion.

PART 3 Charge Distribution

1 Biphenyl compound

1 Dipole moments for the ether group in (A) and the ester group in (B) do not compensate for each other.

2 Dipole moment for the ether group in (C) directs to compensate that for (B).

3 The largest dipole moment occurs in the ester group in (B). The second largest dipole moment occurs in both ether groups in (A) and (C).

2 Fluorene compound

Unsymmetrical structure of charge distribution appears due to the introduction of methylene group. Positive charge was displaced to the methylene group. Therefore, the appearance of weak dipole moment in the fluorene structure can be expected. In fact, a fluorene molecule is known to have a dipole moment[1]. Further, it is confirmed that a fluorene compound has a larger dipole moment than a biphenyl compound, according to dipole moment calculation and by practical measurement.

3 Fluorenone compound

1 Large dipole moment occurs in the carbonyl group of fluorenone structure. This dipole moment is as large as that of the ester group, but is accurately perpendicular to the molecular axis.

2 The dipole moment for the carbonyl group in fluorenone structure and that in the ester group are directed oppositely to compensate for each other.

3 The dipole moment for the ether group, attached to the fluorenone structure and that in the fluorenone structure are directed in the same direction.

PART 4 Polarizability

The polarizabilities concerning the molecular structures (21) and (22) were calculated. The polarizabilites concerning fluorene structure (21) and biphenyl structure (22) are shown in Table 14.

Table 14 Calculated Polarizabilities for Biphenyl (21) and Fluorene (22) Compounds ($Å^3$)

Compound	X	Y	Z
Fluorene (22)	429	202	83
Biphenyl (21)	408	198	75

The X-axis is in the direction of the linkage between oxygen atom and biphenyl or fluorene structures. This direction is almost equal to the molecular axis. Y-axis is equal to the direction, perpendicular to the X-axis on the benzene ring, directly attached to the ether linkage. The Z-axis is on the direction perpendicular to both Y and X-axes. Z and Y-axes are perpendicular to the molecular axis.

Table 14 demonstrates the polarizabilities for the molecular structures (21) and (22) for X, Y and Z axes. Concerning the values for each axis, the polarizabilities for the fluorene structure (22) show greater values than those for the biphenyl structure (21), respectively. Especially, this tendency is distinguished for the values of the X-axis along the

molecular axis.

These results are in fair agreement with the tendency for the deformation polarizabilities Pd (Chapter 6) for the compounds containing these molecular structures. This can be explained as being the result from the π-electron delocalization, due to the fixed two phenyl rings of fluorene structure.

PART 5 Dipole moment

5-1 Biphenyl and Fluorene Compounds

The dipole moments, calculated for compounds (21), (22) and (23), are demonstrated in Table 15. The values on X and Y axes for biphenyl and fluorene compounds cannot be compared directly, because the bond between two phenyl groups in fluorene compound bends about 24 degrees. The X, Y-axis value can be corrected by multiplying by 0.91 (=cos 24°).

Table 15 Calculated Dipole Moments for Biphenyl (21), Fluorene (22) and Fluorenone (23) Compounds (D)

	X	Y	Z	TOTAL
Biphenyl (21)	2.14	1.13	0.92	2.59
Fluorene (22)	1.93	2.08	0.91	2.98
Fluorenone(23)	2.27	3.43	1.56	4.40

X, Y and Z axes demonstrate the same directions as shown in Table 14.

The dipole moment of fluorene compound is larger than that of biphenyl compound. Especially, the Y-axis value is two times larger than that for the biphenyl compound. This difference can be ascribed to the dipole moment in the fluorene skeleton itself, the charge displacement in the structure, as described above. The relationship between the calculated dipole moments is consistent with the measured ones.

5-2 Fluorene and Fluorenone Compounds

Dipole moment of fluorenone compound is larger than that of fluorene compound for X, Y and Z component values. As expected, Y and Z values are especially large. This result confirms that the carbonyl group in fluorenone skeleton increases the dipole moment, perpendicular to the molecular axis.

PART 6 Effects on Behaviors as Ferroelectric Liquid Crystalline Materials

In the following sections, the author will try to explain the behavior as liquid crystalline materials, using the calculated results.

6-1 Smectic A Phase Stability

1 Fluorene compound

Calculated twisted biphenyl structure and increased polarizability of fluorene compound explain stable smectic A phase for a fluorene compound, compared to that for a biphenyl compound, because of the increased intermolecular attractive force due to dispersion force.[2)]

2 Fluorenone compound

Figures 25 and 26 show that the fluorenone carbonyl group is bulkier than the fluorene methylene group (C=O:1.23 Å, C-H:1.11 Å, The increase in molecular width is 0.55 Å, if molecular rotation is presumed.) This explains destabilized smectic A phase.

6-2 Smectic C Phase Stability

1 Fluorene compound

Figures 24 and 25 show that the fluorene compound is rather bulkier than biphenyl compound. Especially, assuming the rotation around a molecular axis, the outboard methylene group increases the molecular excluded volume. In fact, molecules rotate in the smectic C phase. Stability of the liquid crystal phase, in which molecules decline in the layer like smectic C phase, decreases rapidly due to the increase in molecular volume. Therefore, increased volume of fluorene compound destabilizes smectic C phase, in spite of larger polarizability than biphenyl compound.

2 Fluorenone compound

Concerning fluorenone compound, replacing the methylene group in fluorene with carbonyl group increases the molecular width. This is a factor to destabilize smectic C phase. Figure 26 (b) and calculated dipole moment suggest that larger dipole moment occurs by carbonyl group in fluorenone structure. This dipole moment is as large as that of ester group, but almost completely perpendicular to the molecular axis, although the dipole moment for the ester group is declined 36 degrees. This dipole moment for the fluorenone structure is expected to stabilize smectic C phase effectively. In fact, the smectic C phase stability for the fluorenone compound increases.

6-3 Tilt Angles

According to the theory advanced by Van Der Meer and Vertorgen, inductive attraction force, which stabilizes smectic C phase, enlarges a tilt angle.[3] Therefore, a liquid crystalline compound, with large polarizability and dipole moment perpendicular to the molecular axis, is expected to have large tilt angle.

However, a compound with increased molecular width makes it especially difficult to maintain a large tilt angle, because expansive space is necessary for a liquid crystal phase in which molecules decline in the layer.

1 Fluorene compound

Concerning fluorene compound, the following two factors can be considered from the calculation.

1 From calculated polarizability, an enlarged tilt angle is expected.

2 Large molecular width, as shown in Fig. 25, acts to decrease the tilt angle.

Actually, the tilt angle diminished. So, factor 2 is the dominant one for determinating the tilt angle.

2 Fluorenone compound

Increased tilt angles for fluorenone compounds can be explained to be the result caused by large dipole moment of fluorenone structure, expected according to calculation of dipole moment and Fig.26 (b).

References

1 V. Baliah and M. K. Pillay, Indian J. Chem. 9, 563 (1971)

2 W. L. McMillan, Phys. Rev. A4, 1238 (1971)

3 B. W. Van Der Meer and G. Vertogen, J. de Phys., 40, C3-222 (1979)

CHAPTER 8 Second Harmonic Generation Properties of Fluorenone Derivatives

PART 1 Introduction

1-1 Second Harmonic Generation[1)]

Optical polarization P, induced by electromagnetic wave with its electric field E for the observed materials, can be expressed by formula (1).

$$P=\chi^{(1)}E+\chi^{(2)}EE+\chi^{(3)}EEE+\cdots \quad (1)$$

In this formula, $\chi^{(1)}$ is linear susceptibity. $\chi^{(n)}$ $(n\geq 2)$ is n-th nonlinear susceptibility.

When electric field E becomes large, terms higher than the second one cannot be neglected and several kinds of nonlinear optical effects can be observed.

Among these nonlinear optical effects, only the second nonlinear optical effect will be discussed. This effect is called second harmonic generation, SHG. SHG has been the subject of great attention, because half the wave length of light can be generated by irradiation of the light easily generated. For example, 400 nm wave length light can

be obtained, when an 800 nm wave length laser beam is irradiated to the materials, which show SHG. A large variety of usages are expected for this effect. This SHG does not emerge, if the molecular group, which is used as nonlinear optical material, has inversion symmetry. Therefore, for the SHG appearance, molecules must be oriented so as not to show inversion symmetry.

Consider molecules which exhibit nonlinear optical effects. The relationship between optical polarization P and electric field E is expressed by formula (1). A similar relation can be confirmed, concerning isolated molecule. Microscopic polarization p for each molecule can be expanded by local electric field E′, as in formula (2).

$$p=\alpha E'+\beta E'E'+\gamma E'E'E'+ \quad (2)$$

In this formula, α is linear molecular polarizability. β is second order molecular hyperpolarizability and γ is third order molecular hyperpolarizabity. The larger the β value, the greater the SHG.

The SHG appearance is due to the generation of polarization, resulting from the displacement of the

electron cloud around a molecule by an electric field. Displacing π-electrons is easier than displacing σ-electrons. Therefore, large polarization and resulting large SHG can be expected for the molecule with π-electrons.

It is known that β is proportion to the cube of the conjugated chain length[2], and that intramolecular charge transfer is especially effective to increase β[3].

However, the introduction of an intramolecular charge transfer causes the following problem. Intramolecular charge transfer increase β and, at the same time, generates a permanent dipole moment. The generated dipole moments tend to compensate each other. As a result, the molecular group structure becomes inversion symmetrical and, therefore, SHG is forbidden.

Several methods to suppress this inversion symmetry were investigated.

1. Introduction of hydrogen bond to the crystal.[4]
2. Introduction of chiral structure to the molecule.[5]

3.Dispersion of the molecules to polymer matrix and applying an electric field.[6)]

4.Application of liquid crystalline state.[7)]

1-2 Second Harmonic Generation of Fluorene and Fluorenone Derivatives

Previous chapters presented the relationship between molecular structures of liquid crystalline compounds, containing fluorene and fluorenone structure and the properties of liquid crystals, especially ferroelectric liquid crystals.

Moreover, concerning these compounds, optical effects by the typical π-electron systems are interesting, from the standpoints described below.

1.π-electrons are delocalized in wide area.

2.The carbonyl group in fluorenone structure withdraws electrons and works as an electron acceptor. Consequently, charge transfer occurs in the molecule. This charge transfer can be easily confirmed by electronic spectroscopy. (see Chapter 7) The electronic spectrum for the fluorenone compounds differs completely from those of biphenyl compounds and fluorene

compounds. The maximum of the longest wave length peak of fluorenone compound (17) (n=10) is 430 nm, which is 100 nm longer than those for biphenyl compound (18) (n=10) and fluorene compound (16) (n=10). This peak in fluorenone compounds can be assigned to the absorption by intramolecular charge transfer.

3.It is possible to control the molecular group structure in the ferroelectric liquid crystal state. Especially, a structure without inversion symmetry can be made.

From these points of view, SHG for these compounds was observed and interesting information could be obtained, especially for fluorenone compound.

PART 2 Experiment

The SHG measurements were carried out by using Quantel International YG661-10 for Nd-YAG laser, Hamamatsu Photonics R-955 for photomultiplier tube and Sony Tectronics DSA 602 for oscilloscope were used. To observe the samples in liquid crystalline state and liquid state, a Mettler FP 82 heating stage

and FP 80 control unit were used.

YAG laser beam (ca. 100mj/pulse,10pps, 1.06 μm) light was irradiated onto the samples. The obtained SHG (0.53 μm) was detected by photomultiplier tube and the signals were observed by oscilloscope to determine their strength.

Two kinds of samples were used.

A. The fluorene and fluorenone compounds powder across two glass plates.

B. Liquid crystal cells filled with fluorene and fluorenone compounds.

Liquid crystal cells, having a 1x1 cm^2 electrode area, were used. The alignment was made by coating the glass plate surface with polyimide and buffing the surface in one direction. Cell spacing was 2.0 μm, which was obtained by fiber spacers. These compounds are solid at room temperature. They were filled into the cells in liquid state at high temperature (ca. 160°C).

In the case of B, the samples were heated to liquid state and gradually cooled to ferroelectric liquid crystal state and crystal state (-10 °C/min.).

This process was carried out with 30 V electric field and without an electric field. SHG was measured at each state.

PART 3 Result and Discussion

SHG values for samples A vs. urea are shown in Table 16. In the powder states, the fluorene compounds exhibit SHG activity, but fluorenone compounds exhibit no activity.

Table 16 SHG Activity for powder of Fluorene (16) and Fluorenone (17) Compounds (vs. urea)

n	10	12	14
(16)	0.4	0.1	0.7
(17)	0.0	0.0	0.0

In figure 17, SHG for the fluorenone compound in a cell (B) are shown. In the liquid state, SHG was inactive, both with and without an electric field.

However, in ferroelectric liquid crystal state, SHG became active. The activity still remained in the crystal states, although their strength decreased. Through all the states, the values of SHG with electric field are greater than those without electric field.

The X-ray spectrum for the fluorenone compound shows sharp peaks in the powder state. It shows that the fluorenone compound powder is in a microcrystalline state, not in an amorphous state. Therefore, the fluorenone compound powder exhibit no SHG activity, because the crystal structure shows inversion symmetry in the microcrystalline state.

As described in Chapters 6 and 7, the carbonyl group in the fluorenone skeleton shows a large dipole moment. These dipole moments compensate for each other in the crystal and become stable, when molecules are directed anti-parallel. Consequently, the crystalline structure exhibits inversion symmetry and SHG becomes inactive.

Table 17 SHG Activity for Fluorenone Compound (17) (n=10)

State of sample	0 V	30 V
Liquid	0	0
Ferroelectric Liquid Crystal	1	1.3
Solid	0.58	0.73

Fluorene compounds, which do not have strong dipole moment, show SHG activity in the powder state.

In the case of sample B, when the sample was heated to the isotropic liquid state, molecules directed randomly and SHG became inactive. However, when the isotropic liquid was cooled gradually to chiral smectic C phase, SHG became active. The reason is because the dipole moment direction changed and inversion symmetry at π-electrons disappeared in the molecular group. When a 30 volt electric field was applied to the cell, the SHG strength increased. It

seems to be due to the fact that the dipole moment arranged in one direction and the order of molecular group increased.

Furthermore, even though the liquid crystalline state was cooled to crystalline state, SHG activity never disappeared. This means that nonsymmetry, which was generated in the liquid crystal state, remained in the solid state. SHG decreased in the solid state, because polycrystals were formed in the cell. The solid sample formed in the electric field showed larger SHG. It is because the molecular group order was increased by the electric field.

PART 4 Conclusion

Fluorenone compound does not exhibit SHG in the powder state. So, the appearance of SHG seemed to be a structural change in the molecular group. The crystallization from ferroelectric liquid crystal is effective as a method to control the molecular group structure.

Fluorenone compound is effective for SHG, because it has intramolecular charge transfer structure and could control the molecular group

structure, as ferroelectric liquid crystal.

References

1 "Nonlinear Optical Properties of Organic Molecules and Crystals", Eds. D. S. Chemla and I. Zyss, Academic Press, (1987)

2 J. Baden, R. Hierle, A. Perigaud and J. Zyss, ACS Symp. Ser., 233, (D. J. Williams ed.), p.81 (1983)

3 J. L. Oudar and D. S. Chemla, Opt. Commyn. 13, 164 (1975)

4 R. J. Twieg, A. Azema, K. Jain and Y. Y. Cheng, Chem. Phys. Lett., 92, 208 (1982)

5 J. L. Oudar and R. Hierle, J. Appl. Phys., 48, 2664 (1977)

6 K. D. Singer and S. J. Lalama and J. E. Sohn, SPIE Proc. 578, 130 (1985)

7 S. M. Arakelyan, Yu. S. Chilingaryan, G. L. Grigoryan, G. A. Lyakhov, S. Ts. Nersisyan and Yu. P. Svirko, Mol. Cryst. Liq. Cryst., 71, 137 (1981)

Acknowledgement

The author wishes to express his sincerest thanks to Prof. Dr. Ichiro Murata at Osaka University for his unchanged heartful encouragement and appropriate advice during eleven years including the student days.

The author's grateful thanks are expressed to Prof. Dr. Shigetoshi Takahashi for his invaluable directions and heartful encouragement for accomplishment of these studies.

These studies were carried out in Toshiba Corporation R & D Center. The author thanks sincerely his supervisor, Dr. Masanori Sakamoto for his appropriate directions and heartful encouragement. The author thanks Manager Dr. Masayoshi Okamoto at Chemical Lab. for his heartful support to these studies. The author's thanks are expressed to all his colleagues for their useful discussions and cooperations.

Finally, the author thanks his wife, Mariko for her heartful assistance and his parents for their long time support.

October 1991

Publications

Liquid Crystal

1. "Mesophase Transition of Series Materials Containing Fluorene, Fluorenone and Biphenyl Structures with Chiral End Groups"
Mol. Cryst. Liq. Cryst., 164, (1988), 167
K. Takatoh, K. Sunohara and M. Sakamoto

2. "Liquid Crystalline Derivatives Containing Fluorene and Fluorenone Structures"
Mol. Cryst. Liq. Cryst., 182B, (1990), 339
K. Takatoh and M. Sakamoto

3. "Formation and Properties of Ferroelectric Liquid Crystalline Compound Containing -C(O)-S-O- Linkage"
Bull. Chem. Soc. Jpn., 64, (1991), 2270
K. Takatoh and M. Sakamoto

4. "The design of the mesogen structures in ferroelectric liquid crystal molecules"
Kagaku Kogyo, 49 (10), (1989), 881
K. Takatoh and M. Sakamoto

5. "Ferroelectric Liquid Crystals Containing Fluorenone Structure"
K. Takatoh and M. Sakamoto, in preparation.

Miscellaneous

6."Synthesis of a new Weitz-type organosulfur π-donor: 1,2-bis(thioxanthen-9-ylidene)ethene."
J. Chem. Soc., Chem. Commun. 1981, (14), 717
K. Nakasuji, K. Takatoh, M. Nakatsuka and I. Murata

7."Weitz-type organosulfur π-donors with a cumulenic bond. Variation of terminal groups and cumulenic bond in the bis(thiopyranylidene)ethene system."
Chem. Lett. 1982, (11), 1727
K. Nakasuji, K. Takatoh and I. Murata

8."Conversion of
tetrabenzobis(thiopyranylidene)ethene to
a new donor containing a pentalene skelton,
dibenzodithiaacenaphthacenaphthylene, and
their charge transfer complexes.
Chem. Lett. 1986, (5), 829
K. Nakasuji, K. Takatoh, I. Murata, H.
Yamochi, G. Saitoh, T. Enoki and H. Inokuchi